Urban Building Energy and Climate (UrBEC) simulation: Example application and field evaluation in Sai Ying Pun, Hong Kong

Jianxiang Huang [a,b,*], Phil Jones [c], Anqi Zhang [a], Rong Peng [a], Xiaojun Li [c], Pak-wai Chan [d]

[a] Department of Urban Planning and Design, The University of Hong Kong, 8/F Knowles Building, Pokfulam Road, Hong Kong SAR, China
[b] The University of Hong Kong Shenzhen Institute of Research and Innovation, 5/F, Key Laboratory Platform Building, Shenzhen Virtual University Park, No.6, Yuexing 2nd Rd, Nanshan, Shenzhen 518057, China
[c] Welsh School of Architecture, Cardiff University, King Edward VII Avenue, Cardiff CF10 3NB, UK
[d] The Hong Kong Observatory, 134A Nathan Road, Kowloon, Hong Kong

ABSTRACT

The energy performance of a building in a dense city depends to some extent on its surroundings. The impact of the built form, together with anthropogenic heat gains from traffic and building HVAC exhaust, determines external environmental conditions at the Urban Canopy Layer. Existing building energy models are limited in accounting for micro-scale variations of the urban microclimate, which may significantly modify a building's energy performance in density cities. This paper presents the Urban Building Energy and Climate (UrBEC) model, a coupled urban microclimate model (UMM) and building energy model (HTB2) developed to assess the time varying energy performance of a cluster of buildings and the combined heat gains to the external space from direct and reflected solar radiation, traffic and the exhaust from HVAC systems in a high-density city. The simulation results were evaluated by comparison with field measurement data collected from the Sai Ying Pun neighbourhood in Hong Kong, on a summer and winter day. Predicted and measured air and surface temperature at the four locations were found to be in reasonable agreement. Simulation results indicate an average of 1-3 ºC of temperature rise in street canyons compared with the ambient air in summer. Street level air is predicted to be 0.6 ºC warmer than those at higher levels (20m +). Anthropogenic heat from traffic and building HVAC exhaust are the dominant contributors to temperature rise in street canyons in summer, exceeding the contribution from urban surfaces. The predicted building cooling demand is expected to increase up to 15 % in summer due to the warming effect in street canyons. The UrBEC model runs significantly faster than current CFD-based approaches. Therefore, the model has the potential to support early stage design and planning decisions in a dense city.

1. Introduction

A building and its surrounding urban microclimate are highly interdependent in a high-density city, such as Hong Kong. Overshadowing by neighbouring buildings affects solar radiation incident on a building's façade; temperature fluctuations of external wall surfaces modify external long-wave heat exchanges; breezeways and relatively sheltered areas affect the ability of the urban area to exhaust heat gains and pollutants. This interdependency alters a building's energy performance and the performance of neighbouring buildings. There are also anthropogenic heat gains from traffic and HVAC exhaust that, together with the solar gains and urban surface heat transfer, contribute to external heat build-up, generally referred to as the Urban Heat Island (UHI) effect. Research literature reports that air temperatures in street canyons can typically rise by 4–6 ℃ above those of the rural areas in Hong Kong, a high-density city [1], which will affect a building's energy performance as well as external pedestrian comfort and the use of outdoor spaces [2]. Hong Kong's buildings are also found to cause the 'wall effect' [3] which uplifts localized air temperature and stagnates airflow [4]. To fully understand a building's thermal and energy performance one should therefore consider a building in the context of its neighbouring buildings and urban microclimate, and the combined heat gains to the external space from direct and

reflected solar radiation, traffic and the exhaust from HVAC systems.

This need to understand the interdependency of buildings with their microclimate calls for a new approach to the energy and environmental modelling of buildings within an urban cluster. In practice, most buildings are not designed to operate in the actual surrounding microclimate. Generally, models such as EnergyPlus [5], Ecotect [6], or IES VE [7] do not normally account for the immediate local microclimate. Instead, designers rely on weather data measured at remote rural stations which usually differ considerably from those of an urban site. Some take into account the urban climate effect at city-scale through generalised modifications to standard weather data to uplift temperatures [8]. However, they do not account for the combined modifying effect of solar radiation, air temperature and wind flow. Urban climatology models have been developed at city-scale (>1km) [9], but this is not particularly useful for the design of individual buildings in their immediate urban context. This gap in energy modelling is critical at the scale of building clusters and the space in-between (50–500 m), which applies to most city planning and development projects.

Despite the apparent needs in practice, only a few attempts were identified in the research literature to model interactions between urban microclimate and building energy performances [10]. The Computational Fluid Dynamics (CFD) method is the primary tool applied in urban microclimate analysis [11,12]. For instance, Yang et al. [13] coupled EnergyPlus and ENVI-met, a CFD simulation software [14], to assess building energy performance in urban environments. Bouyer et al. [10] developed a coupled simulation model based on ANSYS Fluent, another CFD software. A primary drawback of CFD-based models, despite great merits, are the relative slow running speed and difficulties to link with other simulation platforms [15]. Many consider CFD models unsuitable to assess large districts and complex urban configurations over an appropriate time period [16]. Recent urban energy assessment tools such as CitySim [17], UMI [18], and the software package Design-Builder in combination with EnergyPlus [19] have made significant progress in the assessment of overshadowing effects of buildings; yet both assume homogeneous air temperature in the urban environment, which may limit their application for Asia's high-density cities with significant anthropogenic heat gains and the urban canyon effects. The authors have conducted preliminary work on an integrated model of urban microclimate and building energy. Results were reported in the proceedings of the Building Simulation 2017 conference [20].

This paper presents the development of the Urban Building Energy and Climate (UrBEC) simulation model, which couples the multizone urban microclimate airflow network model (UMM) with the building energy model (HTB2). The models exchange air and surface temperature data at an hourly basis. The UrBEC model also includes the consideration of anthropogenic heat gains from traffic and exhaust from building HVAC systems. The model is able to predict variations in urban surface and air temperatures both spatially and over time, which can then be related to building energy use and external comfort. The building energy model HTB2 has been developed to simulate large numbers of buildings simultaneously using Sketch-Up [21] to quickly set up the various input files that describe the buildings, layout, construction, HVAC systems, occupancy and weather data, with plugins for calculating solar shading from neighbouring buildings, topography and landscape features [22]. The Urban Microclimate Model (UMM) [23] uses a multizone airflow network model to assess canopy layer airflow in high-density cities, where air mass flow within an interconnected network of external zones is driven by pressure and density differences. Results have been evaluated using a field experiment conducted in the Sai Ying Pun Neighbourhood in Hong Kong, one of the densest cities in the world.
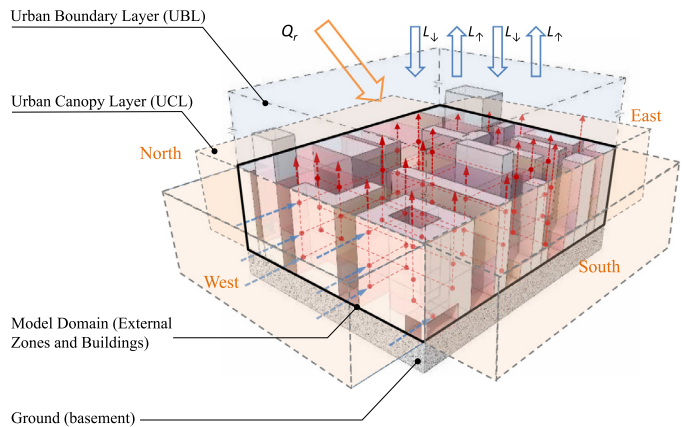

Fig. 1. Schematic depiction of the urban microclimate model.

2. Theory and methods

The Urban Building Energy and Climate (UrBEC) simulation model is based on the dual-component of (1) the Urban Microclimate Model (UMM) [23] and a (2) the Building Energy Model (BEM) HTB2 [22]. The UMM provides localized external zone air temperatures to HTB2, while external building surface temperature and HVAC exhaust data, calculated by HTB2, are returned to the UMM on an hourly time step. Field evaluation studies were conducted in Sai Ying Pun, a high-density neighbourhood in Hong Kong. Details on simulation set-up such as model domain and the boundary condition are introduced.

2.1. A multizone model for urban microclimate

The Urban Microclimate Model (UMM) is based on a multizone airflow network approach [23] developed to assess the mass and energy of the air in urban environments. The zonal approach was first developed to describe indoor environments [24] and later applied for outdoor spaces [25]; the model can be used to assess a high-density urban environment in which wind-driven airflow is weakened by buildings and the movement of air is restricted to a limited number of street canyons. The model domain, the space within the study site between the ground and building roof, is divided into a series of semi-enclosed 'zones' resembling roof-less buildings (Fig. 1). The volume of air within the domain exchanges mass and energy with each zone's surrounding urban surfaces, anthropogenic heating/cooling sources. To simplify the process, it is assumed that the airflow is driven by pressure, temperature and density differences, upholding the conservation of mass and energy, while relaxing the momentum conservation equations. It is assumed that this relaxation method is appropriate for high-density cities where wind-driven flow are often stagnant, at which time buoyancy flow dominates [16]. The model domain is joined by external boundaries from above, the east, south, west and north. Details on boundary conditions are provided in Section 2.3.1. The UMM model has been developed and evaluated using a mock-up site with satisfactory agreement between predicted and measured data [26].

2.1.1. Zonal mass conservation & airflow equations

The air within each zone is characterized by a uniform temperature (T_i) and density (ρ_i). The zonal air pressure (P_i^e) at any given height (H_e) is expressed as $P_i^e = P_i^c - \rho_i g H_e$ (1) according to the principle of the stack pressure [27], where P_i^c is the air pressure at the geometric centre of the zone, and H_e is the vertical distance from the zone centre. Pressure, temperature, and density observe

the ideal gas law $\rho_i = P_i/R_{air} T_i$ (2) (R_{air} is the gas constant) [27]. The airflow rate F_{ij} from zone i to neighbouring zone j is a function of pressure and density differences at the border and characteristics of the openings $F_{ij} = f[\Delta P_{ij}, \Delta \rho_{ij}, A_{ij}]$ (3). Mass conservation is observed at each zone $V_i \frac{\partial \rho_i}{\partial t} + \sum_{j=1}^{J} F_{i,j} = 0$ (4). Since mass changes caused by density difference is often negligible, we have $\sum_{j=1}^{J} F_{i,j} = 0$ (5). Airflow models calculating the F_{ij} and F_{ji} are provided in the authors' earlier work [23].

2.1.2. Zonal energy conservation

The energy conservation equation for the body of air within zone i is expressed in formula (6), which describes heat transfer from solid surfaces, airflows to and from neighbouring zones, thermal massing, and anthropogenic heat generation, i.e. traffic and HVAC exhaust:

$$0 = \sum_{k=1}^{K} hA\left(T_k^{surf} - T_i\right) + \sum_{a=1}^{A} \lambda q_a^{gen} + \sum_{j=1}^{J} C_p F_{ji}\left(T_j - T_i\right) + \frac{\partial T_i}{\partial t} C_p \rho_i V_i \tag{6}$$

where K is the number of enclosing solid surfaces, each with the surface temperature of T_k^{surf}; h is the convective heat transfer coefficient between solid surfaces and air; T_k^{surf} is the temperature for each solid surface; A is the number of active heat sources within zone i, q_a^{gen} and λ are the power and operational coefficient of each heat source; F_{ij} and F_{ji} are the airflow rates between zone i and neighbouring zone j; J is the number of neighbouring zones; C_P and V_i are the specific heat capacity and volume of the zonal air.

2.1.3. Convergence criteria

The system reaches an equilibrium if airflows, pressures and temperatures converge across all the cells of the solution domain. Thus, the solver for the UrBEC model works iteratively following a three-loop structure:

- In Loop A, zonal temperatures were taken as given, zonal pressure P_i and inter-zonal airflow F_{ij} are calculated by iteratively solving the pressure balance and airflow equations (Eqs. (3)–(5)) at a small time-step, convergence is reached if the pressure residual ΔP, defined as the maximum differences of P_i between iterations, drops below a pre-set threshold.
- In Loop B, zonal pressure and inter-zonal airflow were taken as given, the air temperature of each zone T_i was solved iteratively in small time-steps using Eq. (8). Convergence is achieved if temperature residual ΔT drops below a predefined threshold.
- In Loop C, the zonal air temperature T_i computed in Loop B above was input in Loop A again to calculate the new inter-zonal airflow F'_{ij}. The results reach convergence only if the maximum difference between F'_{ij} and F_{ij}, or the flow residual ΔF, drops under a predefined threshold.

2.2. Building energy model – HTB2

The external surface temperatures, heating and cooling energy demand, and exhaust from air conditioning equipment are modelled dynamically for an urban cluster of buildings using HTB2 and VirVil SketchUp (Jones et al.), both were developed at the Welsh School of Architecture, Cardiff University. HTB2 is typical of the more advanced numerical models developed over thirty years and extensively tested and validated by the IEA Annex 1 [28], IEA task 12 [29] and the IEA BESTEST [30]. HTB2 uses as input data, hourly climate for the location, building material properties and construction details, spatial attributes, HVAC system settings, and occupancy profiles, to calculate the energy required to maintain specified internal thermal conditions [31]. Due to its advantages of flexibility and ease of modification, HTB2 is well suited for use in the field of energy efficiency and sustainable design of buildings. VirVil SketchUp is an extension HTB2 developed for urban scale modelling. By linking SketchUp with HTB2, it can pre-process and carry out dynamic thermal simulation for multiple buildings in a community or urban scale, with plugins developed to calculate the shading masks for each façade, or part of, that describe overshadowing from neighbouring buildings and topography.

2.2.1. Surface energy model

The urban surface temperature T_i^{surf} is computed by solving the energy balance equation in which energy conservation is observed among solar/long-wave radiation, convection, conduction, and thermal massing as shown in formula (7) below

$$0 = E_i A_i + U_i\left(T_b - T_i^{surf}\right) + h\left(T_i - T_i^{surf}\right) + \frac{1}{2}\varepsilon\sigma\left(T_i^{mrt4} - T_i^{surf4}\right) + \frac{\partial T}{\partial t} C_i M_i \tag{7}$$

where E_i is the incoming solar radiation at surface i; A_i is the solar absorption coefficient of the surface material; U_i is the surface heat transmission coefficient; T_b is internal temperature inside the building or the underground soil; h is the convective heat transfer coefficient; T_i is the localized air temperature at surface; ε and σ is the surface emissivity and Stephan-Boltzmann's constant; T_i^{mrt} is the mean radiant temperature at the surface; $\frac{\partial T}{\partial t}$ is the surface temperature changes during each time-step; M_i and C_i is the mass and material specific heat capacity of the surface. The solar radiation falling on a building surface is predicted in HTB2, using a shading mask which breaks the sky viewed from the external surface into 324 (9×36) blocks of 10 by 10 degrees. An unconditioned building space (basement) is created underneath and in contact with the ground in order to compute the ground surface temperature.

2.2.2. HVAC exhaust model

Heating and cooling energy demand at each time step is modelled for all building zones by considering the internal, ventilation, solar and fabric gains. To simplify, each building is considered as a single thermal zone in HTB2 with a simple temperature set point T_b. Q_b is the energy demand required by the heating or cooling system as it is expressed in formula (8):

$$Q_b = Q_{li} + Q_{sp} + Q_{oc} + r_{ex} C_b M_b \left(\bar{T}_{ext} - T_b\right) + \sum_{i=0}^{k} U_i\left(T_i^{surf} - T_b\right) + \frac{\partial T}{\partial t} C_b M_b \tag{8}$$

where Q_{li} is the heat gain from lighting; Q_{sp} is the heat gain from small power, i.e. electric light and appliances; Q_{oc} is the heat gain from occupants according to schedule; r_{ex} is the air exchange rate of the building under mechanical or natural ventilation; M_b and C_b is the mass and specific heat capacity of the air inside the building. $\bar{T}_{ext}$ is the mean air temperature of external zones that surround the building weighted by wall surface area; T_b is the building internal temperature according to the set point. U_i is the average heat transmission coefficient at surface i among a total of k surfaces, weighted by the area of glazing and wall surfaces. T_i^{surf} is the temperature of surface i among a total of k surfaces. $\frac{\partial T}{\partial t}$ is the room temperature changes during each time-step t.

HVAC exhaust q_b^w is calculated based on predicted cooling energy demand from HTB2 as it is shown in formula (9) below:
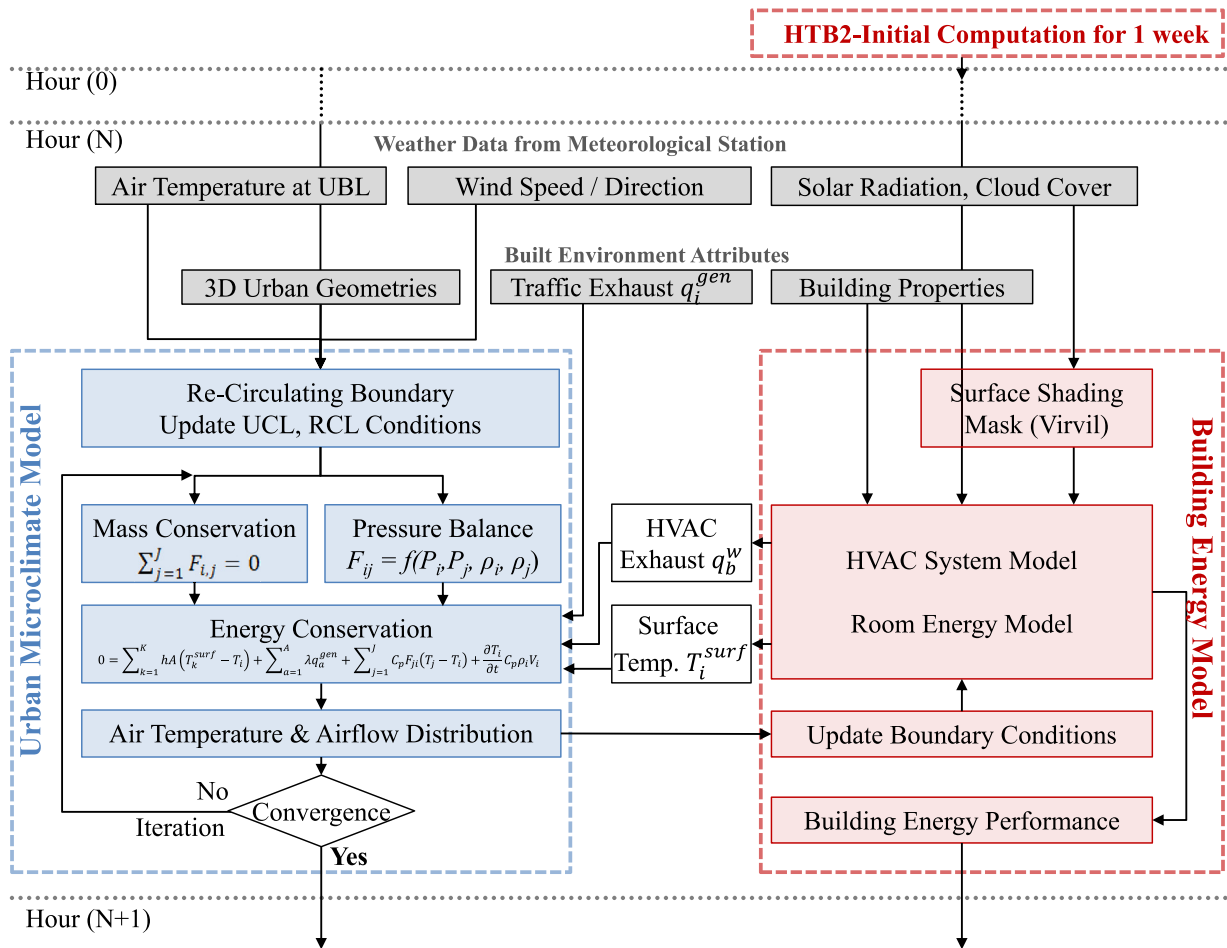
$$q_b^w = |Q_b| + \frac{|Q_b|}{COP} \tag{9}$$

HTB2-Initial Computation for 1 week

Hour (0)

Hour (N)

Weather Data from Meteorological Station

| Air Temperature at UBL | Wind Speed / Direction | Solar Radiation, Cloud Cover |

Built Environment Attributes

3D Urban Geometries | Traffic Exhaust q_i^{gen} | Building Properties

Urban Microclimate Model

Re-Circulating Boundary
Update UCL, RCL Conditions

Mass Conservation
$\sum_{j=1}^{J} F_{i,j} = 0$

Pressure Balance
$F_{ij} = f(P_i, P_j, \rho_i, \rho_j)$

Energy Conservation
$0 = \sum_{k=1}^{K} hA\left(T_k^{surf} - T_i\right) + \sum_{a=1}^{A} \lambda q_a^{gen} + \sum_{j=1}^{J} C_p F_{ji}(T_j - T_i) + \frac{\partial T_i}{\partial t} C_p \rho_i V_i$

Air Temperature & Airflow Distribution

No / Iteration — Convergence — **Yes**

HVAC Exhaust q_b^w

Surface Temp. T_i^{surf}

Building Energy Model

Surface Shading Mask (Virvil)

HVAC System Model

Room Energy Model

Update Boundary Conditions

Building Energy Performance

Hour (N+1)

Fig. 2. Conceptual strategy for the Urban Building Energy and Climate (UrBEC) simulation model.

where Q_b is the building cooling demand calculated by HTB2; *COP* is the Coefficient of Performance for cooling. For heating operations in cold seasons, q_b^w is a function of ventilation exhaust and heat recovery. For the case study of Sai Ying Pun, a predominantly residential district, such facilities do not apply since domestic heating is rare under Hong Kong's subtropical climate. The *COP* for Hong Kong's residential air conditioner ranges between 2.3 and 2.9 according to the Electronic and Mechanical Service Department of the Hong Kong Government (EMSD) [32], the median value of 2.6 was used. In the context of this study for a residential neighbourhood where decentralized window AC units are common, q_b^w is assumed to be discharged to external zones surrounding the building proportional to the surface area of each wall.

2.3. Coupling HTB2 with UMM

Fig. 2 below shows the strategy of coupling UMM and HTB2. At the completion of each time-step, HTB2 passes updated values of the building surface temperatures to UMM. It also sends data on building HVAC exhaust, if any, that is then input to the external zones. At this point HTB2 pauses. UMM then computes a new set of temperatures for the external zones, which it passes to HTB2. Then HTB2 proceeds with the next hour. At each hour both models are updated with weather data from a local station, and UMM is updated with hourly data for traffic heat gains.

The main modification to HTB2 is the reference to outdoor air temperature. Instead of each external wall, window, roof element and the indoor zone relating to a single external air temperature taken from the weather file, it uses the individual outdoor zones

set up by UMM. These zones will have increased or decreased temperature values in comparison to the weather data file, depending on the urban canyon effect and anthropogenic heat. The modification of UMM, is that it takes HTB2 building external surface temperatures, rather than calculating them internally. The ground surface temperature is calculated as a wall element in HTB2, similar to calculating internal ground floors, the 'roof' being the external ground. They have direct solar gains and shading applied to their external surface, as any other external wall or roof element.

2.3.1. Boundary conditions

The model domain is covered by the Urban Boundary Layer (UBL) from above; the east, south, west, and north boundaries are joined by the Urban Canopy Layer (UCL) of adjacent urban neighbourhoods, or the Rural Boundary layer (RBL) if the site is surrounded by a rural context. Aside from temperature and pressure boundary conditions from UBL, UCL or RBL, the model also takes into account thermal boundary of urban surfaces, i.e. and anthropogenic heat from traffic and building HVAC systems.

The Temperature Boundary conditions at the Urban Boundary Layer (UBL) above the model domain can be represented by measurement data from urban weather stations. These data are usually made available for metropolitan areas, where roof-top weather stations are set up to monitor urban weather conditions. However, if the model domain is situated in an urban context surrounded by the urban canopy layer (UCL), which is more complex and cannot be easily measured due to the spatial variation of temperature profiles. A re-circulating boundary method has been developed in this study to simulate conditions for UCL; details are in Section 2.3.2.

The Pressure Boundary for external wind is calculated from both static and dynamic pressure. The static atmospheric air pressure (P_i^s) at the edge of an external zone i is determined by the gravity stacking effect of. P_i^s and can be expressed in Formula *Error! Reference source not found.*), where P_0 is the atmospheric pressure measured from the weather station, ρ_{air} is the density of air; g is the gravitational constant; h_i is the height of the geometric center of zone i from the height of the weather station.

$$P_i^s = P_0 - \rho_{air} \, g \, h_i \qquad (10)$$

The dynamic air pressure (P_i^d) at the windward surface of zone i is a function of the incoming wind speed and direction. P_i^d can be expressed by Formula **Error! Reference source not found.**) below, where θ is the incident angle of wind from the normal direction of the zonal surface. ρ_{air} is the density of air, V_h is the wind speed adjusted to height h according to the vertical distribution profile.

$$P_i^d = \frac{1}{2} \cos \theta \, \rho_{air} \, V_h^2 \qquad (11)$$

Surface Temperature Boundary at building surfaces and the ground is calculated using the Building Energy Model HTB2 at an hourly resolution. The areas of shared surfaces adjacent each external zones are calculated using Rhinoceros, a 3D modeling software. The surface temperature of glazing is not accounted for given the relatively small window-to-wall ratio (<0.2) on the field study site for residential buildings.

Anthropogenic Heat Gains from traffic and HVAC systems are modeled hourly. Urban traffic is treated as linear heat source along vehicular roads; the intensity of heat generation is estimated using traffic count data, fleet composition, types of fuel, etc. HVAC exhaust from buildings are treated as point sources; the intensity of HVAC exhaust for each building is estimated using the HTB2 building energy model, which is then distributed to external zones according to the location of exhaust outlets. Details are provided in Section 2.4.6 and 2.4.7.

2.3.2. Re-circulating boundary

When modelling the thermal performance of an urban block, the boundary conditions need to be established, including wind speed and air temperatures. As the urban block is located within the city, its boundary conditions will be different from the weather station values. In this simulation a recirculating boundary method has been used to account for the upwind conditions immediately neighbouring the solution domain.

The re-circulating boundary applies a N-step process to estimate temperature conditions for the East, South, West, and North boundaries. The input data is the measured weather data from UBL.

- In the first step, air temperatures for the East, South, West, and North boundaries are set to equal those of the Urban Boundary Layer at the top. The UrBEC model is used to solve for preliminary zonal air temperature within the model domain. The mean zonal temperature within the domain is calculated to be $\overline{T_1}$.
- In a second step, $\overline{T_1}$ is then used to substitute temperature conditions for East, South, West, and North boundaries. The UrBEC model is executed again to obtain results of $\overline{T_2}$..
- In step N, $\overline{T}_{N-1}$ is used to substitute temperature conditions for East, South, West, and North boundaries, the procedure repeat itself until $\overline{T}_N$ converges. In other words, $\Delta \overline{T}_N = (\overline{T}_N - \overline{T}_{N-1}) < 0.02°C$, the threshold of equipment accuracy.

The number of steps (N) appreciate for the Re-Circulating Boundary calculation depends on the size of the boundary offset (L_B) relative to the size of the model domain (L_D). If the model domain is surrounded by urban context that is sufficiently large ($L_B / L_D \approx \infty$), the steps N needed should be large enough to allow $\overline{T}_N$

to converge. Alternatively, the step N should be determined by the size of the boundary offset from the model domain to the Rural Boundary Layer as it is illustrated in Fig. 3 below.

2.4. Field evaluation studies

Field experiments were carried out in Sai Ying Pun, a high-density neighbourhood in Hong Kong. The aim is to evaluate the predicted localized external zone air temperature and building façade surface temperature.

2.4.1. Site

The study site consists of 9 urban blocks giving a total footprint area of 252m by 378m in size at the centre of the Sai Ying Pun neighbourhood (22° 48' N, 114° 24' E, altitude 4 m). The average Floor Area Ratio (FAR), the ratio between total building floor area and the site area, equals 9. The site consists of high-rise residential towers some 100m in height, while along streets there are apartment buildings that are 20m-tall. The neighbourhood is served by four major vehicular roads: Des Voeux Road West and Queen's Road West stretch from east to west, Eastern Street and Centre Street connect south to east. Four locations were selected for urban microclimate measurements, each one varies considerably in urban layout, and intensity of anthropogenic waste heat. Fig. 4 shows the overall site and the location of four measurement locations: A,B,C and D. A is on the sidewalk of Des Voeux Street, a main busy street with 4-lane vehicular traffic. B is at the road intersection between the Western Rd. and Queen's Rd. West; C is in Sai Yuen Lane, a narrow alleyway inside the residential block. D is at the end of Chung Ching Street. The street width, density and configurations vary among the four sites, providing a potential variation in microclimate conditions.

2.4.2. Field study schedule

Measurements were conducted on a cool winter day (Dec. 9, 2014) and a hot summer day (Sept.6, 2015).

Given the hot and humid subtropical climate, window air conditioning units are a common household feature in Hong Kong, while space heating is rarely used during the mild winter period. Exhaust from building HVAC systems is expected to be significant during Hong Kong's hot summer, yet negligible during the mild winter. The weather was sunny or partially cloudy on both study days. Measurement data were collected between 08:00 and 22:00 on each study day. Data for late evening and early morning were not collected due to logistic constraints. Traffic data were recorded manually by researchers on the 4 major vehicular roads. A summary of the weather conditions on both study days can be found in Table 1.

2.4.3. Instrumentation

Air temperature and wind speed were measured concurrently at the four locations at 1.5 meters above ground using four HOBO portable weather stations; specifics of the component sensors were provided in the Appendix. Building surface temperatures were measured using an infrared camera (FLIR E40-NIST) at hourly intervals. Photographic images were analysed using TESTO IRSoft software, in which the mean surface temperature for each building wall was calculated using the Polygon Region Average (PRA) tool provided by the software. A fixed emissivity value was used (0.97) for building façades including both concrete walls and glazing area, since the window-to-wall ratio is relatively small (< 20%) on the study site. Fig. 5 illustrates the calculation of the average surface temperature for all the pixels within the polygon drawn over the building wall for the summer period. Pixels of air conditioning units, which are usually warmer than the wall surface by 10 °C, are excluded from the calculation using the histogram plot method. A
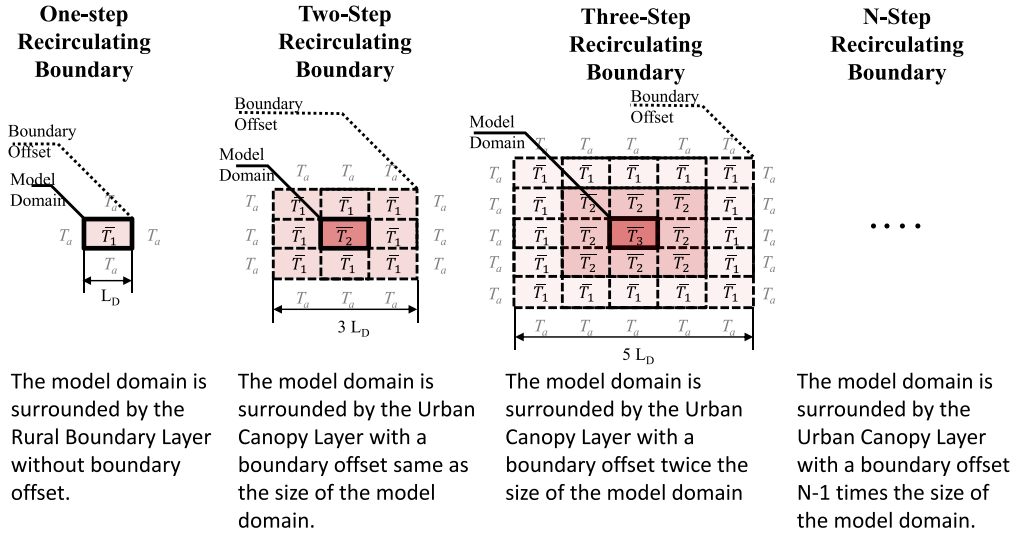
One-step Recirculating Boundary

The model domain is surrounded by the Rural Boundary Layer without boundary offset.

Two-Step Recirculating Boundary

The model domain is surrounded by the Urban Canopy Layer with a boundary offset same as the size of the model domain.

Three-Step Recirculating Boundary

The model domain is surrounded by the Urban Canopy Layer with a boundary offset twice the size of the model domain

N-Step Recirculating Boundary

The model domain is surrounded by the Urban Canopy Layer with a boundary offset N-1 times the size of the model domain.

Fig. 3. The steps needed in Re-Circulating Boundary calculation in relation to the size of the boundary offset in proportion to the model domain. Diagrams are drawn in plan view.

Fig. 4. (Upper) The Sai Ying Pun area of 252 m by 378 m and 4 measurement locations drawn on top of Google Earth imagery. (Lower) Site photos for the 4 locations with measurement equipment highlighted in yellow.
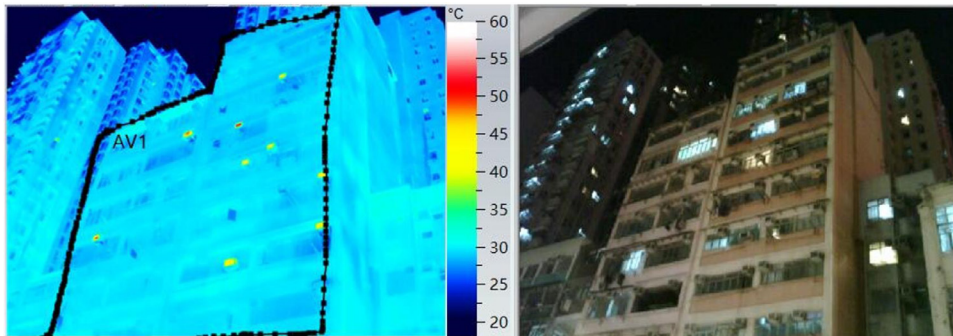
Fig. 5. Measurement of building surface temperature using infrared thermography at 278 Des Voeux Road West. (Left) infrared thermography with manually drawn polygon delineating the area of a building wall; (right) the same building under photographic camera; both images were taken at 20:24 Sept.6, 2015. Onsite ambient air temperature was 30.3 ºC at the time of the survey.

Table 1

Weather data measured from nearby weather station network from the Hong Kong Observatory on Dec. 9, 2014 and Sept.6, 2015.

	Dec.9, 2014 0:00 – 23:00	Sept.6, 2015 0:00 -23:00
Air Temperature (°C)		
Mean	19.5	29.6
Standard deviation	1.2	1.3
Minimum	17.9	28.1
Maximum	22.0	32.3
Solar Radiation (W/m2)		
Mean	289.3	439.8
Standard deviation	275.8	377.4
Minimum	0.0	0.0
Maximum	694.4	941.7
Wind Direction (° from North)		
Prevailing wind direction (PWD)	90°	280°
% of hours deviate from PWD	50%	50%
Average Wind Speed (m/s)*		
Mean	5.7	2.2
Standard deviation	1.7	1.8
Minimum	2.3	0.1
Maximum	8.4	4.8

* wind speed was adjusted to the reference height of 10m above ground.
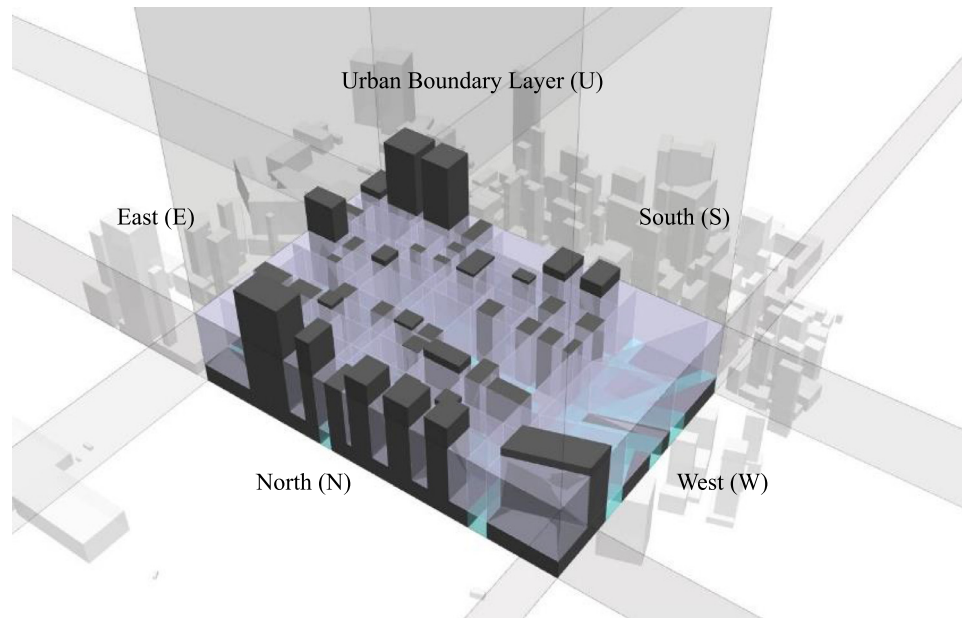
Fig. 6. 3D building and external zone geometry input and boundary conditions for urban microclimate model.

limitation of our approach is that the infrared imagery was usually not taken perpendicular to the target surfaces due to limits of access in a dense urban site;

2.5. Simulation set-up

To prepare for simulation of the Sai Ying Pun neighbourhood, 3D building geometries and external zones were delineated in the model domain; weather data were collected from 6 nearby weather stations as input data for boundary conditions; traffic data were collected manually on-site during the two study days (one weekday and one weekend day); building parameters, e.g. window-to-wall ratio and solar absorption coefficient of surface materials, were estimated based on field surveys.

2.4.4. Model domain configuration

The UrBEC model was applied to simulate conditions on the study site in Sai Ying Pun. The model domain consists of a rectangular cuboid of 300 m x 200 m x 100 m in dimension (length/width/height). The 3D building geometries and spaces have been manually divided into 191 external zones and 41 buildings as shown in Fig. 6. The criteria for manual division is to ensure external zones are simple, concave polyhedrons, which can be represented by conditions at the geometric centre. The external zones were grouped into two vertical layers at the height of 0-20 m and 20-100 m above ground; the former represent the air volume at the street level, while the later represents those above. Fig. 7 shows the building geometry data for HTB2 building energy simulation.

2.4.5. Boundary condition inputs

In order to account for model boundary conditions, hourly weather data were collected from the Hong Kong Observatory's network of 83 ground-based weather stations. Fig. 8 shows the location of the 6 nearest ground-based weather stations, all within 5 km from the study site.

- The air temperature profile of the urban boundary layer was collected from the Hong Kong Park Station (22°16′42"N,
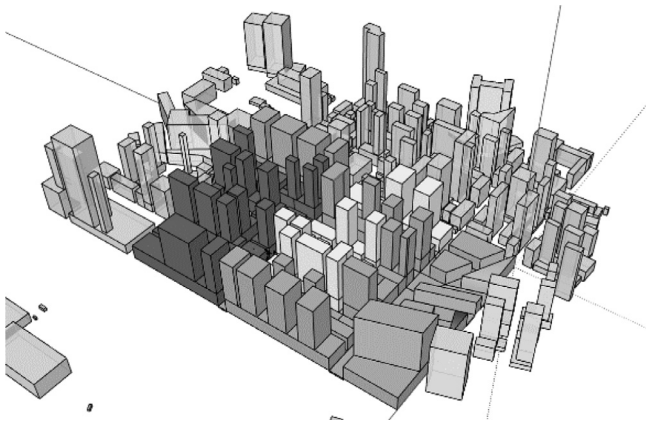
Fig. 7. 3D building geometry input for HTB2 building energy model.

114°09′44″E). The station is situated in an elevated urban park at 26 m above sea level, and it is 2.7 km windward from the study site.

- Wind speed and direction data were taken from the Star Ferry Station (22°17′35″N, 114°10′07″E) 3 km windward from the study site, the closest weather station with anemometers deployed.
- Solar radiation data were measured from the King's Park Station (22°18′43″N, 114°10′22″E), the closest one with pyranometer sensors.

A two-step Re-Circulating Boundary condition is used in the simulation of SYP study site (Fig. 10). The choice of step N=2 is de-

termined by the boundary offset appropriate for the Sai Ying Pun neighborhood, a narrow strip of urban context bonded by the Victoria Harbor to the North and the wooded hills to the south. A two-step boundary offset the size of the model domain ($L_B = 3\ L_D$), as it is shown in Fig. 9 below, appears to have reached the Victoria Harbor to the North and the wooded mountain range to the South.

2.4.6. Traffic exhaust inputs

Heat Input from Traffic exhaust were calculated from vehicular traffic data collected onsite. Vehicle count and fleet composition were manually counted on 4 major roads onsite during the two study days. The number of vehicles by vehicle types were recorded on hourly basis. Heat generation from traffic exhaust q_i^{gen} for zone i can be expressed as a function of vehicle count, fleet composition, vehicle heat mission rate, and road length within the zone. Hence, q_i^{gen} was calculated using Formula (12) below

$$q_i^{gen} = \frac{L_i}{3600} \sum_{m}^{M} N_m Q_m \tag{12}$$

where L_i is the length of road in zone i (m); N_m is the hourly vehicle count for each vehicle for category m, which were manually recorded for four major road Des Voeux Road West (example in Fig. 11), Western Street, Third Street, and Queen's Road West. M is the number of categories for vehicle types: (1) Car (sedan, van, SUV), (2) Minibus, (3) Truck, (4) Bus. Q_m is the linear heat emission rate per vehicle along road (W/m) which can be expressed as a function of fuel consumption rate and heat of combustion for fuel per vehicle (Table 4). All fuel energy was assumed to be discharged to the ambient environment as sensible heat, includ-
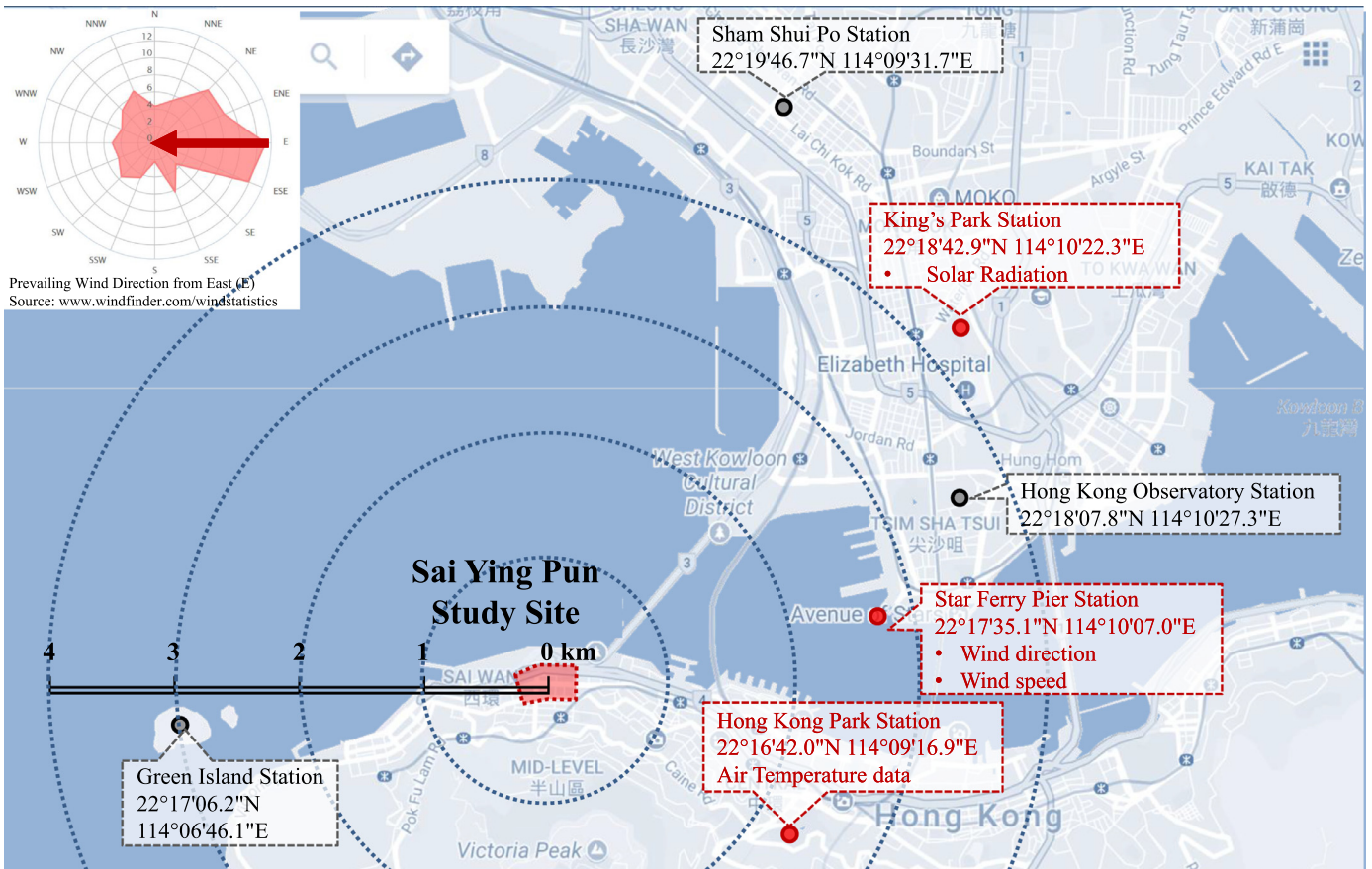
Fig. 8. The Sai Ying Pun study site in relation to 6 nearby ground-based weather stations within the distance of 5 km (source: Google Map & HKO).

Fig. 9. The choice of a two-step boundary offset for the study site in Sai Ying Pun, Hong Kong.
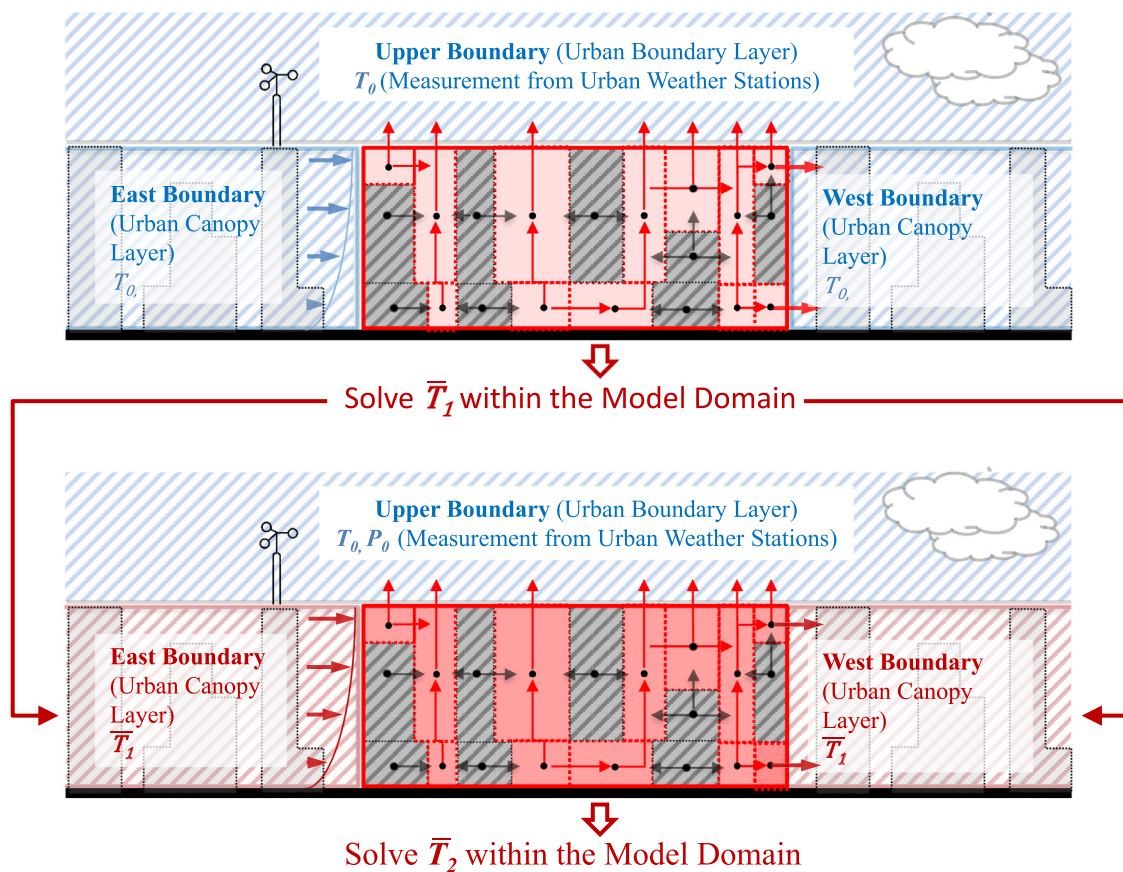
Fig. 10. The re-circulating boundary methods applies a two-step process to estimate temperature conditions for surrounding Urban Canopy Layer.

ing engine exhaust, vibration, and kinetic energy which dissipate in vehicle braking, tire and mechanical abrasion. Q_m was calculated using Formula (13): where F_{m0} is the fuel consumption per 100km travelled (given by vehicle types in Table 2); ρ_m is fuel density (0.83 kg/L for diesel, 0.76 kg/L for gasoline); H_m is the heat of combustion for fuel (45 MJ/kg for diesel, 47 MJ/kg for gasoline).

2.4.7. Building parameters

The indoor ventilation rate is set to equal 0.5 in reference to the average figure from field measurement conducted in Hong Kong [33]), while the intensity of small power equipment, such as lighting, computers, and home appliances is set to equal 7.5 W/m^2. The non-occupancy hours are set to be from 9:00 – 18:00 on weekdays
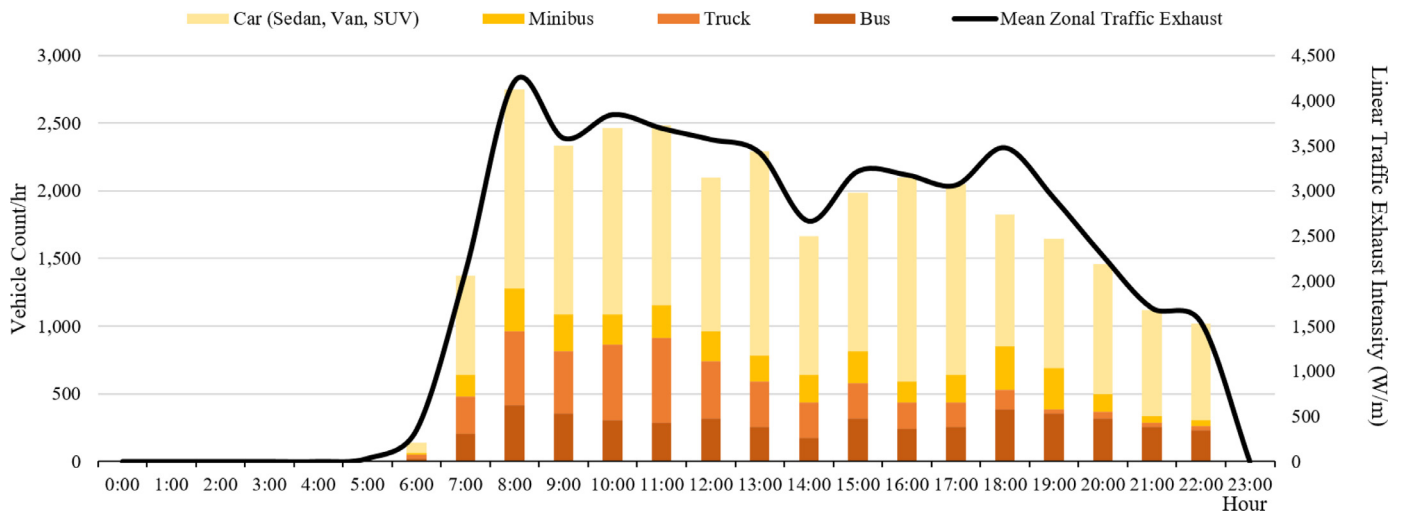
Fig. 11. Hourly traffic exhaust and vehicle count by vehicle type on Des Voeux Road West on Dec.9, 2014.

Table 2
Vehicle types and fuel consumption data used in this study.

Vehicle Type	Fuel Consumption per 100 km (L)
1. Car (Sedan/Van/SUV)	14.0 (Gasoline)
2. Minibus	17.7 (Diesel)
3. Truck	20.0 (Diesel)
4. Bus	66.2 (Diesel)

on which the HVAC systems are turned off. The material property data were obtained from a site survey and used as input for HTB2 building energy model. The Solar Absorption Coefficient (SAC) of building walls is set at 0.7 (light concrete), while those of the roof and ground is set to equal 0.3 (light painted concrete) and 0.8 (asphalt).

3. Results and analysis

Predicted zonal air temperature and surface temperature are compared with measured data. Results depict a profile of temperature and airflow in street canyons. Sensitivity studies showed the contribution to the warming effect of street canyons from building HVAC exhaust, traffic and the urban canyon effect (solar radiation).

3.1. Field evaluation

There was a satisfactory agreement between the predicted and measured zonal air temperature at location A, B, C, D as observed for the two study days (Figs. 12 and 13). The UrBEC model has been used to simulate the time varying air temperatures in a district of a high-density city as well as the temperature differences across different locations. Of note is the agreement between pre-

Fig. 12. Predicted and measured zonal air temperature at four measurement locations (A, B, C, D) represented in red, green, yellow and blue accordingly; measurement in solid line; simulated data in dashed line) with weather station air temperature (solid grey line) on Sept.6, 2015.
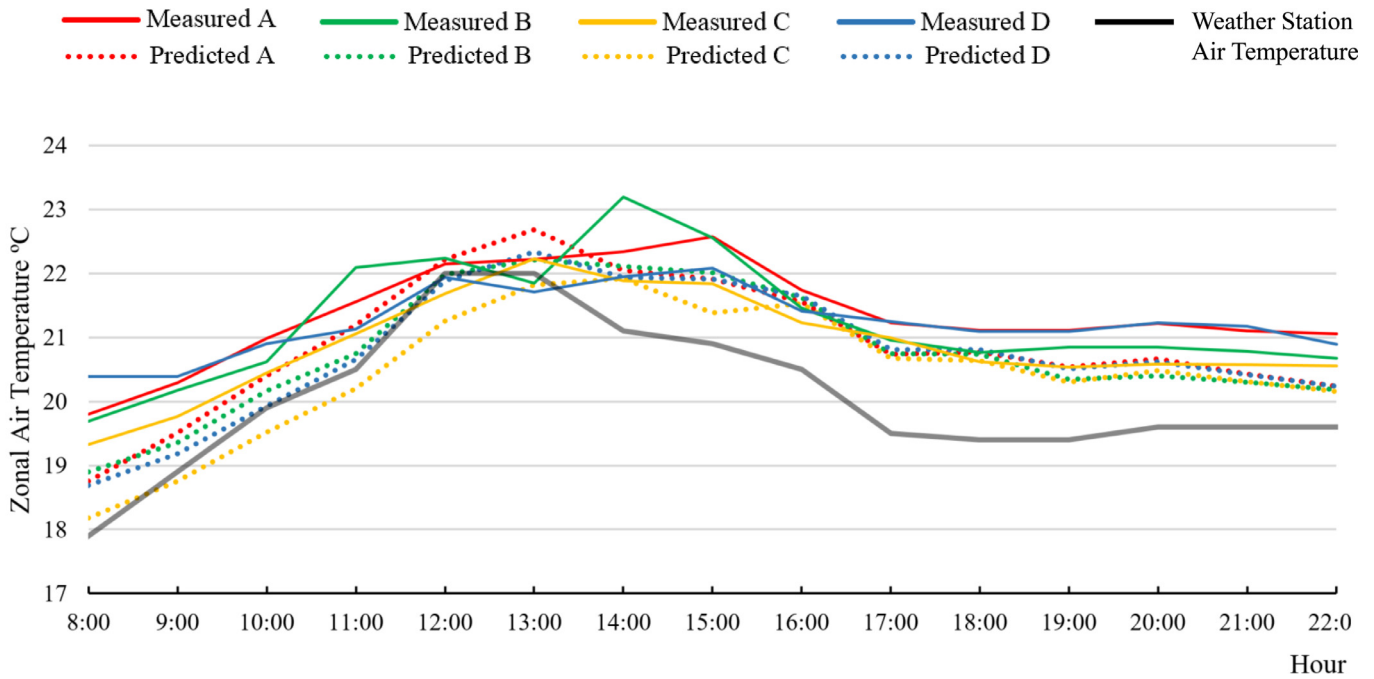
Fig. 13. Predicted and measured zonal air temperature at four measurement locations (A, B, C, D) represented in red, green, yellow and blue accordingly; measurement in solid line; simulated data in dashed line) with weather station air temperature (solid grey line) on Dec.9, 2014.
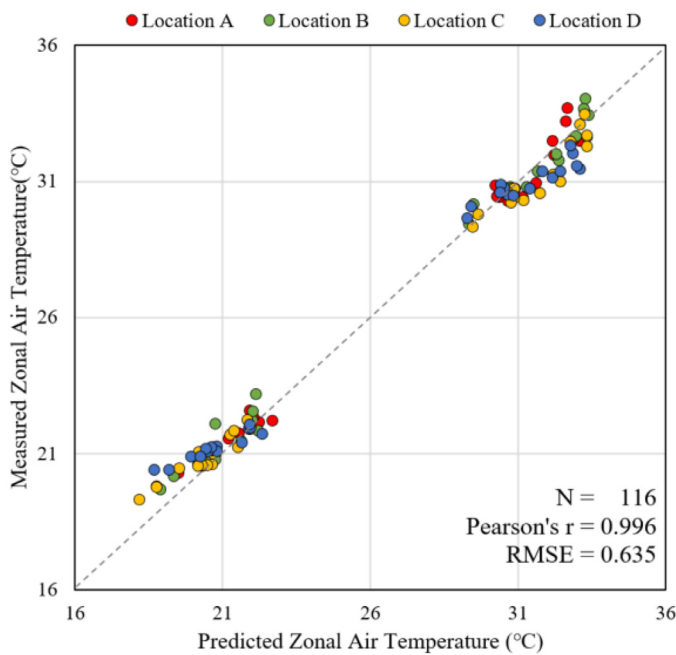
Fig. 14. Measured and prediction zonal air temperature at 4 locations on Dec.9, 2014 and Sept.6, 2015.

dictions and measurements of the delay in peak daily zonal temperatures compared to the air temperature at the weather station. A Pearson's r of 0.996 and a Root Mean Square Error (RMSE) RMS of 0.635 °C were observed between the predicted and measured data (Fig. 14). Differences between simulated and measured zonal air temperature are normally distributed, with a mean difference of −0.10 °C.

The model has slightly over-predicted zonal air temperature by 0.27 °C in summer, and under-predicted by 0.45 °C in winter (Fig. 15). A potential cause for the difference could be due to un-

certainties associated with field measurement in a real urban site, in which anthropogenic heat sources such as cooking or other domestic activities are difficult to account for precisely (Fig. 16).

A reasonable agreement between predicted and measured surface temperature was observed in both summer and winter (Fig. 17). Predicted and measured data are closely correlated with each other (Pearson's r = 0.985; RMSE = 0.634 °C). Differences between the two are normally distributed; Overall, the model appeared to have overestimated surface temperature in summer (by 0.31 °C) and winter (by 0.48 °C) (Fig. 17).

3.2. Warming effect in street canyon

The model has predicted a complex profile of temperature distribution across the Sai Ying Pun study site. Fig. 18 indicates the range of zonal temperatures in the model domain for a 3-day period in summer. Air temperatures inside the street canyons are predicted to be between 1–3°C higher than those of the Urban Boundary Layer measured from a nearby weather station. The average difference is around 2 °C, while the peak difference could be nearly 4 °C in the time range of afternoon and early evening. The capacity to assess zonal temperature profile allow planners to assess the quality of thermal environment in urban pocket parks and major street corridors (Fig. 19).

Model results also suggest a decreasing air temperature profile upwards in the domain. Air temperatures at the lower lever zones (below 20 m) is on average 0.5 °C higher those at the higher level (20–100 m). The vertical distribution of temperature implies that pedestrians are exposed to hotter air at street level; also, households occupying the lower levels of a residential buildings (0-20 m) experience higher outdoor temperature compared with residents at higher levels. Given the "positive floor-level premium" on real-estate property market where wealthier households often occupy higher floor levels in a residential building in Hong Kong [34], the vertical temperature distribution suggest inequalities of UHI exposure for those dwelling at the lower floor levels and hence the less wealthy households.
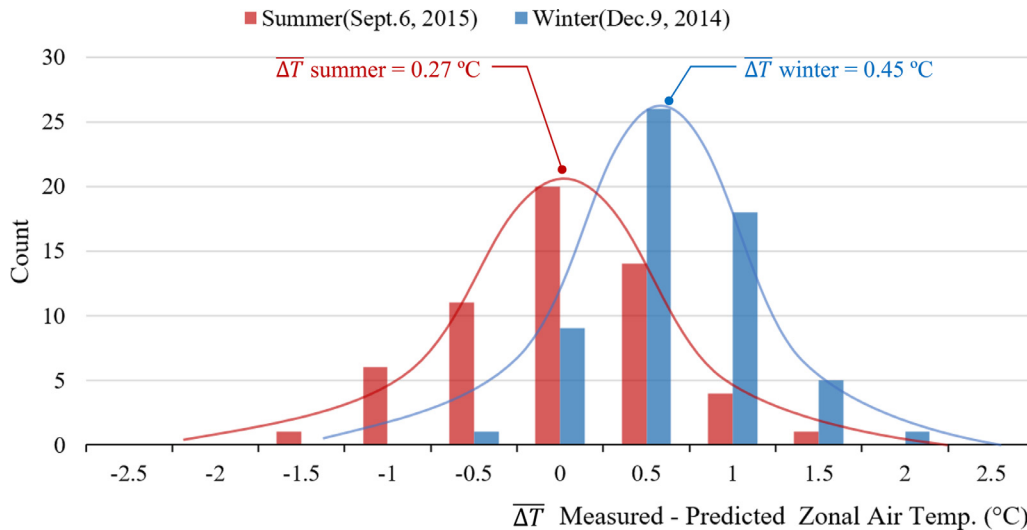
Fig. 15. Distribution of differences between predicted and measured zonal air temperature in summer and winter. The model appeared to have over-predicted zonal air temperature by 0.27°C in summer and under-predicted by 0.45°C in winter.
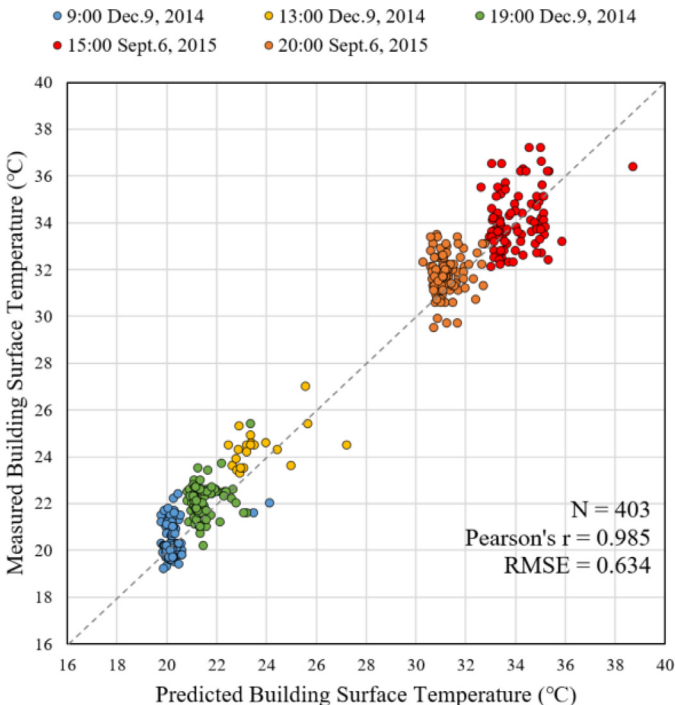

Fig. 16. Measured and predicted mean surface temperature for building façades on Dec.9 2014 and Sept.6 2015.

Predicted surface temperature variations follow closely behind those of the ambient air temperature (Fig. 20). The peak median surface temperature appears at 15:00 h, 2 h behind those of the peak solar radiation, presumably due to the thermal mass of buildings and the ground. The range of surface temperatures widen with days of more intense solar radiation, with unshaded roof surface temperatures peaking above 55 °C.

3.3. Sensitivity study

A sensitivity study was conducted in order to estimate the independent thermal contributions to the UHI, from the urban canyon effect (solar radiation), traffic exhaust, and HVAC exhaust. Simulation were conducted for 3 scenarios for: (1) *Real-World* scenario with all 3 thermal contributors in place; (2) *No Traffic Exhaust* in

which traffic waste heat was removed from model inputs; (3) *Ghost Town* where both traffic and HVAC exhaust were removed from model inputs. Simulations were run for a 15-day period in both summer (Sept. 4 – 19, 2015) and winter (Dec.7 – 22, 2014). A summary for the 3 scenarios and the model domain set up is shown in Fig. 21. Temperature profiles of the street canyons were assessed using the average zonal temperature of the core block at the centre of the site, consisted of 16 buildings and 31 external zones at the street level. This allows for proper control of boundary condition assumptions on air temperature, wind, and solar shading from nearby buildings. Results of the sensitivity study are plotted in Fig. 22 (winter) and Fig. 23 (summer).

Fig. 24 shows the hourly temperature profile inside street canyons and contributions from urban canyon effect, HVAC and traffic exhaust. Temperature values are calculated for the core site zones over a 15-day period. It appears that on average, the urban canyon effect (from solar) creates a thermal lag combined with a slight increase in peak temperature, whilst the traffic and HVAC exhaust cause an increase in the peak temperatures. On average, in winter (Fig. 24 left) the peak temperature uplift is just under 1°C and in summer (Fig. 24 right) it is just over 1 °C.

The results suggest anthropogenic heat appears to be the dominant contributor of temperature rise in summer on the study site, exceeding those from the urban canyon effect. Fig. 25 shows hourly sensible heat transfer to the urban canopy layer at the core block in Sai Ying Pun from surface conduction, traffic and HVAC exhaust for a 15-day period in summer; values are normalized by the footprint area of the core block. Traffic exhausts contributes up to 140 W/m^2 (24 h average 79 W/m^2); contribution from building HVAC system is between 40-80 W/m^2 (24 h average 61 W/m^2). Heat gain from urban surfaces dips down to -30 W/m^2 between 6:00 – 13:00 and rise up to 40 W/m^2 in the afternoon (14:00 – 20:00), suggesting building walls and the ground are cooler than the air during morning yet warmer in the afternoon.

The heat gains from surfaces is lower than those of the HVAC and traffic exhausts. This finding is supported by the surface temperature data in Fig. 5, where the wall temperatures were measured to be typically 1 to 2 °C higher than the ambient air temperature of 30.3 °C. This would indicate a surface heat transfer from the wall surface to the outside air of around 6 W/m^2, which is similar to the value reported in Fig. 25 at 20:00 h

The above findings differ from previous literature [35], which rank anthropogenic heat of lower importance than solar heat gains
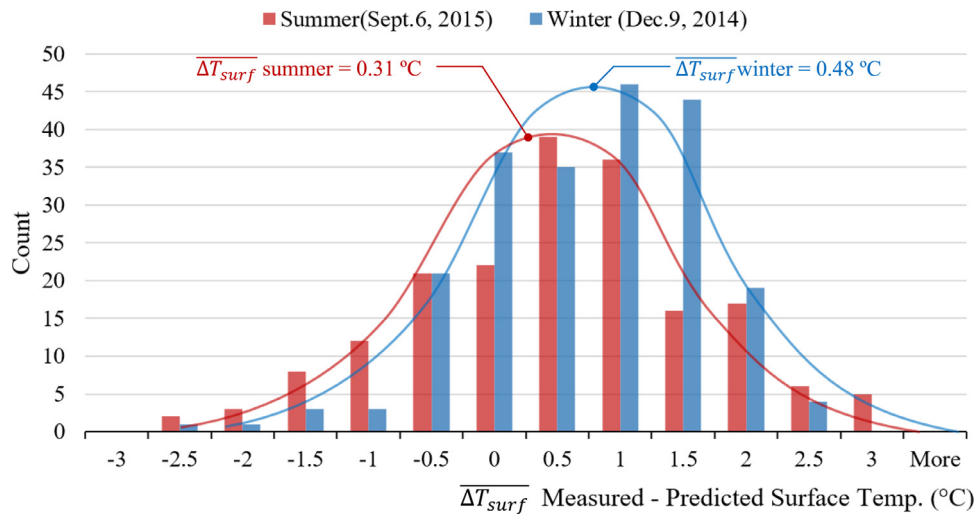
Fig. 17. Distribution of differences between predicted and measured surface temperature in summer and winter. The model appeared to have overestimated surface temperature in summer by 0.31°C and winter by 0.48°C.
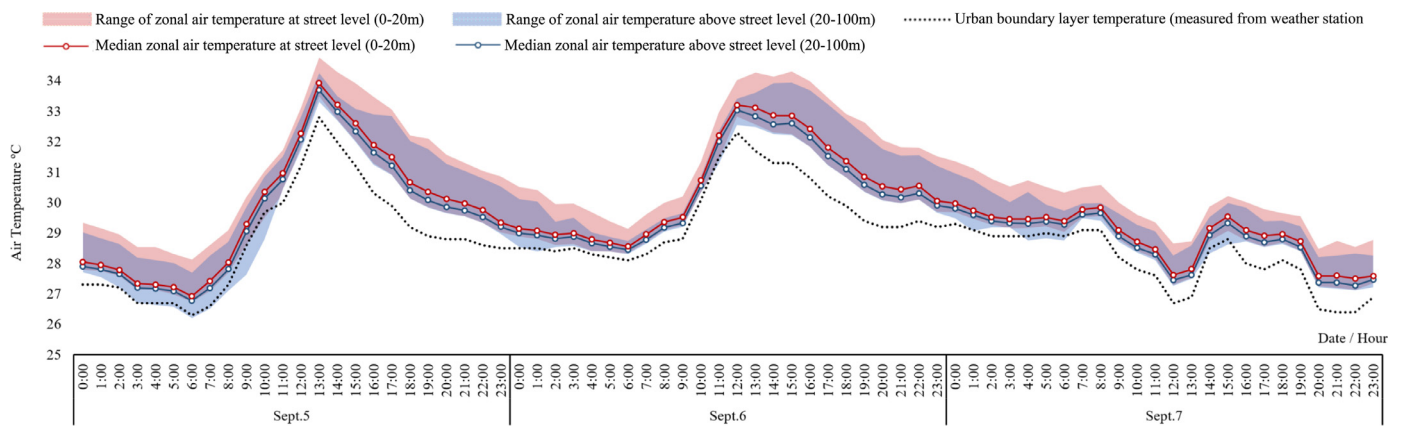

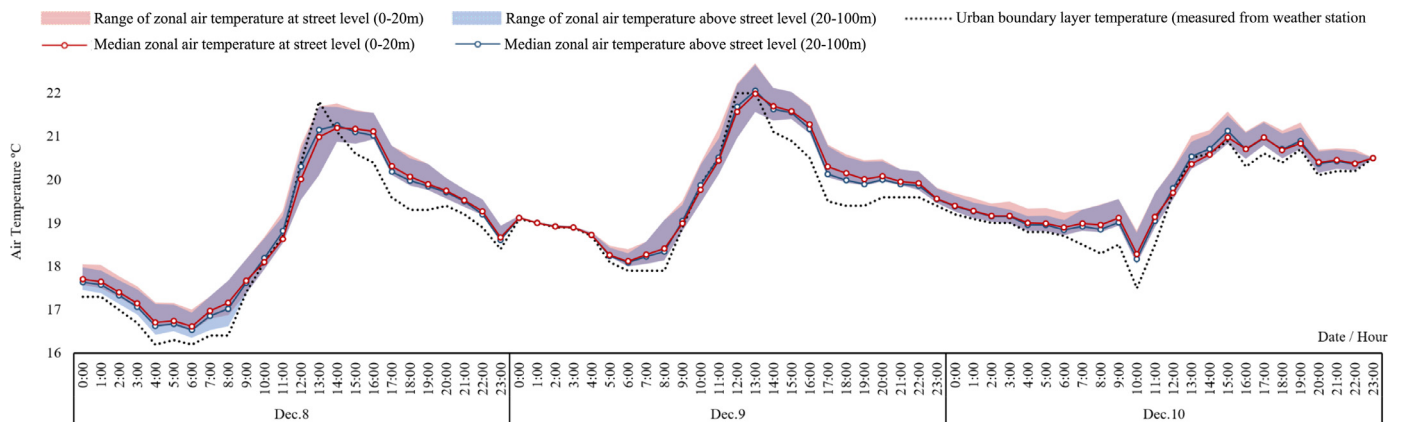**Fig. 18.** Predicted zonal air temperature profile in summer (Sept.5-7, 2015).

Fig. 19. Predicted zonal air temperature profile in winter (Dec.8-10, 2014).

and vegetation in terms of contribution to UHI. Possible explainations are (1) the roof surfaces of Hong Kong's dense high-rise urban form prevented the bulk of solar radiation from penetrating down to the street canyons; (2) the anthropogenic heat is intense due to the shear density of traffic, buildings, occupants and activities. The results also shed light on UHI mitigation measures in high-density cities. Aside from current policy priorities such as surface albedo, greenery and improvement of urban air ventilation [36], Hong Kong might consider mitigating anthropogenic heat

emission in street canyons in summer, i.e. reduce vehicular traffic, encourage electric vehicles, or replace window AC units with district cooling system.

3.4. Impact of urban microclimate on building energy

The UrBEC model is able to predict the building energy demand based on temperature profiles of the building's immediate surroundings. Fig. 26 presents the predicted cooling demand for
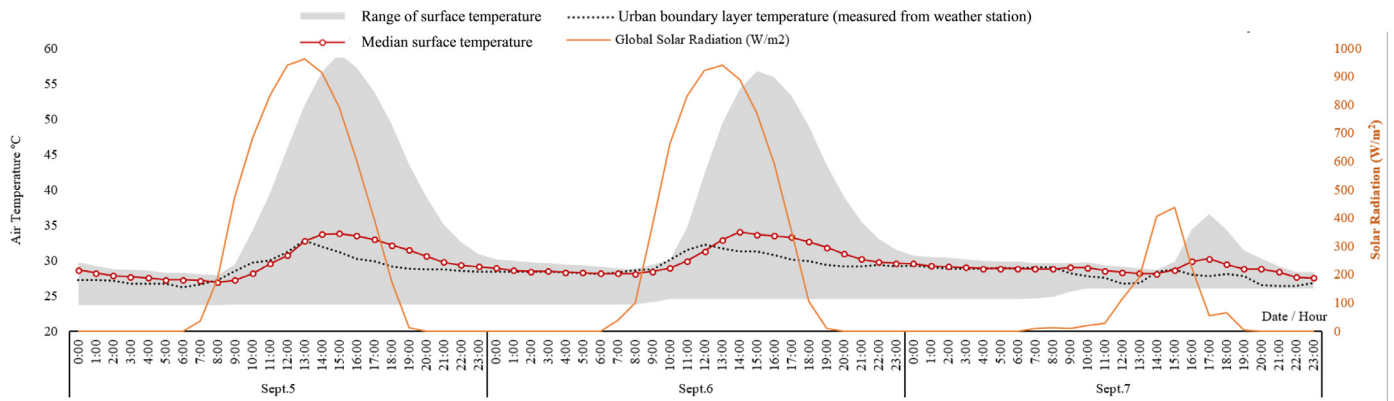
Fig. 20. Predicted surface temperature profile in summer (Sept.2015) in comparison with solar radiation.
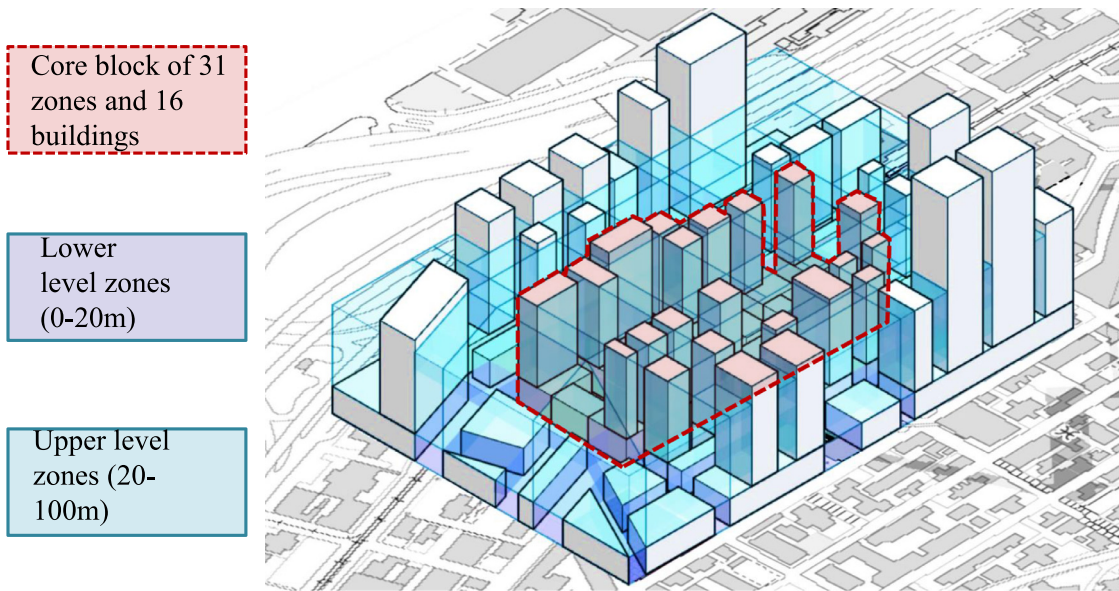

Fig. 21. Summary of simulation scenarios and model domain set-up for the sensitivity study; the core block consisted of 31 zones and 16 buildings at the centre of the domain is highlighted in red.

16 buildings at the core block in summer. Predicted mean building cooling demand using the UrBEC model is 13.8 W/m², 15% higher in comparison to predicted energy demand based on Virvil-HTB2 (12.2 W/m²) based on the assumption of a uniform temperature across the site. The results suggest the necessity of accounting for localized urban temperature variation in building energy simulation in a high-density city, where the interactions between a building and its context can lead to considerable variability in microclimate.

3.5. Convergence and computing

Convergence of the UrBEC model was satisfactory. The residuals for Loop A (pressure), Loop B (temperature), and Loop C (flow rate) are plotted in Fig. 27 for a total of 30 days (720 h) of simulation run in both winter (Dec. 7–26, 2014) and summer (Sept.4-23, 2015). The above results are achieved using a self-developed solver algorithm written in Python programming language. The time step values used for Loop A, B are 3.5×10^{-6}s and 0.07s, respectively. The convergence criteria for pressure is 0.0065 Pa, 2×10^{-4} ºC for temperature, and 100 kg/s for flow rate, which translates into a homogeneous airflow of 0.2 m/s for a street opening 20 m by 20 m in size, within the precision level of measurement equipment used in this study. The pressure residual ΔP, temperature residual ΔT, and flow residual ΔF, decreased below their threshold levels.

An advantage of the UrBEC model lies in its computing speed. On average, it takes 10 min to execute a simulation run for an hour, 5 times faster than the state-of-the-art tool such as FLUENT and 20
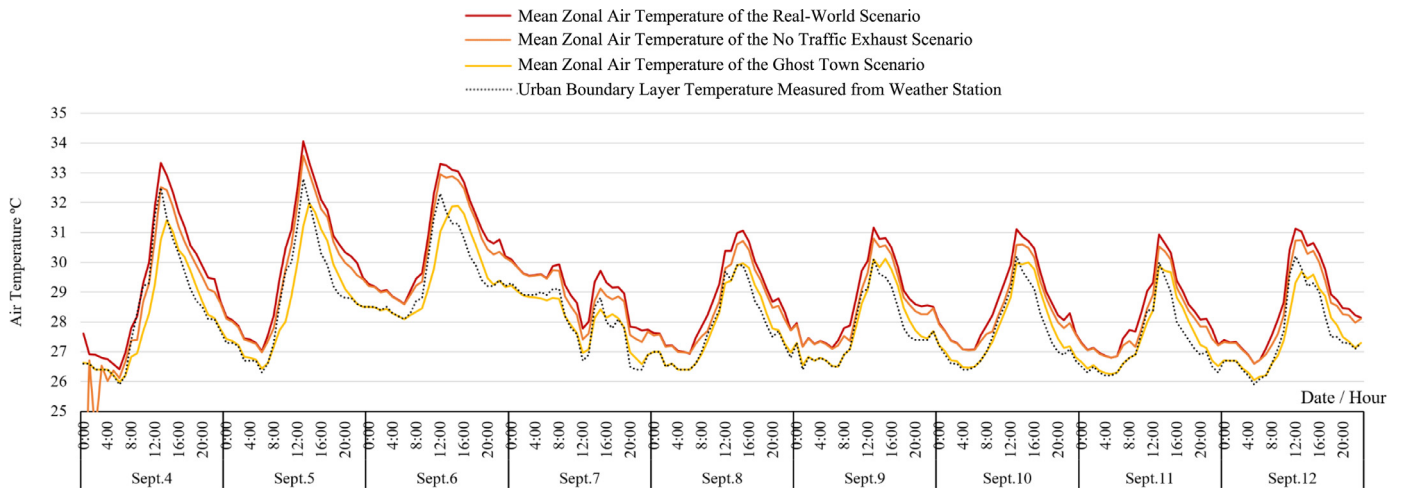
Fig. 22. Predicted mean air temperature of the core zones for the Real-World, No Traffic Exhaust, Ghost Town scenarios for the first 9 days of the 15-day period in Sept. 2015. Air temperature from the Urban Boundary Layer measured from weather station is plotted in the dashed line.
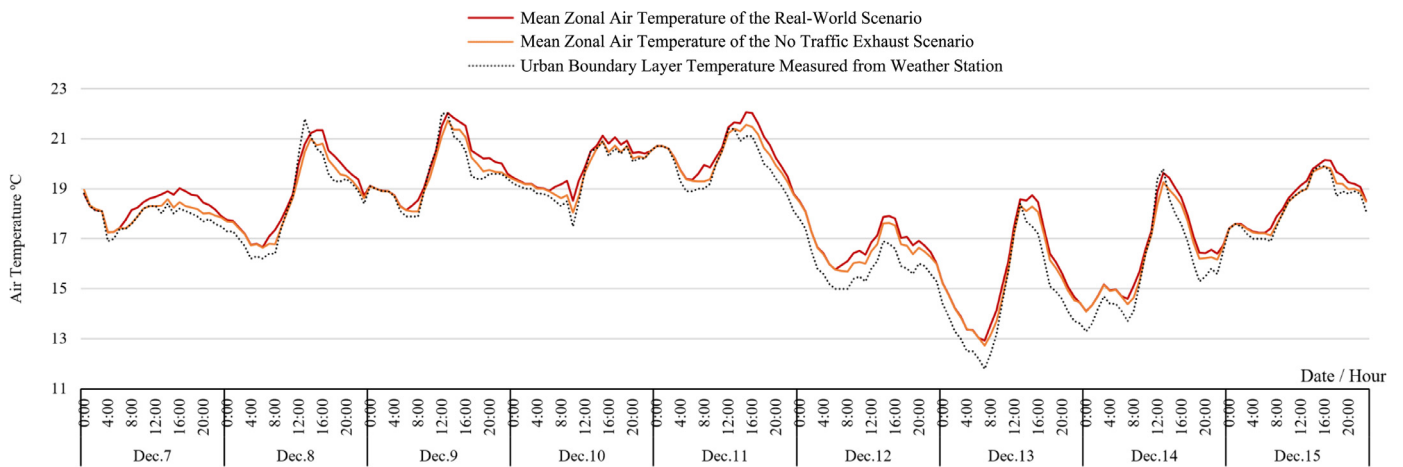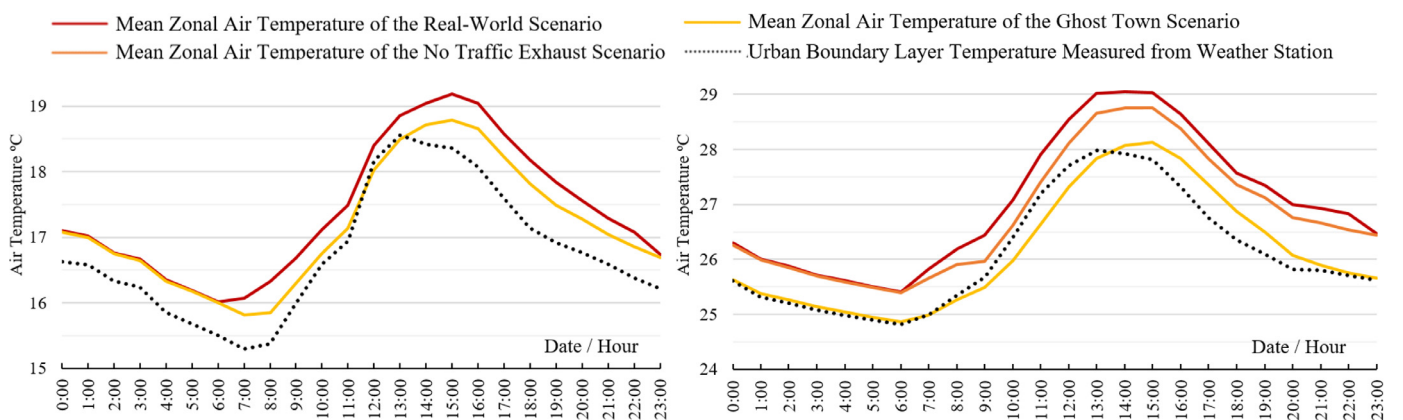

Fig. 23. Predicted mean air temperature of the core zones for the Real-World, No Traffic Exhaust, Ghost Town scenarios for the first 9 days of the 15-day period in Dec. 2014. Air temperature from the Urban Boundary Layer measured from weather station is plotted in the dashed line.

Fig. 24. Predicted 15-day average hourly temperature profile under alternative scenarios in winter (left) and summer (right).

times faster than ENVI-met based approach. At the moment, the UrBEC model runs on Python and Fortran programming languages, which, if streamlined in a single programming language platform, can be accelerated further. It is expected to be able to simulate annual-hourly conditions for days in the next steps.

3.6. Limitations and next steps

This paper summarizes progress of an on-going research project over the course of 4 years. Major limitations lie three-fold below, mostly related to practical constraints of model evaluation studies
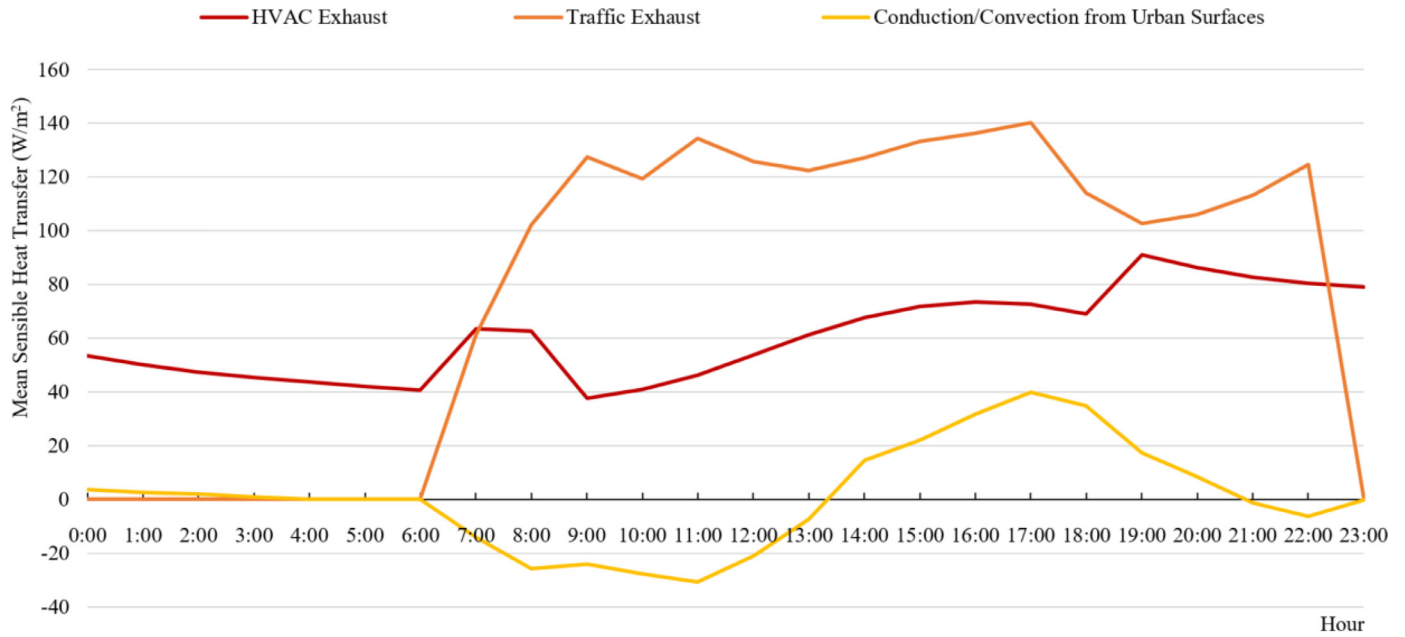
Fig. 25. Sensible heat transfer to urban canopy layer on the study site from HVAC exhaust, traffic exhaust, and urban surfaces in summer over a 15-day period in summer (Sept. 4-19, 2015); results are divided by the footprint area of the core block (31,636 m^2).
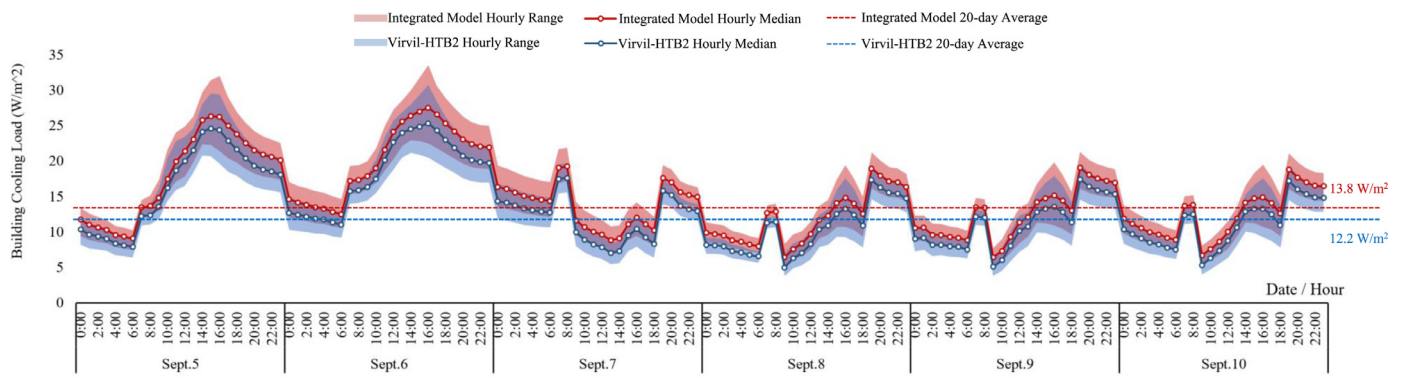

Fig. 26. Predicted building cooling demand for a sample of 16 buildings at the core block using the UrBEC model and Virvil-HTB2.
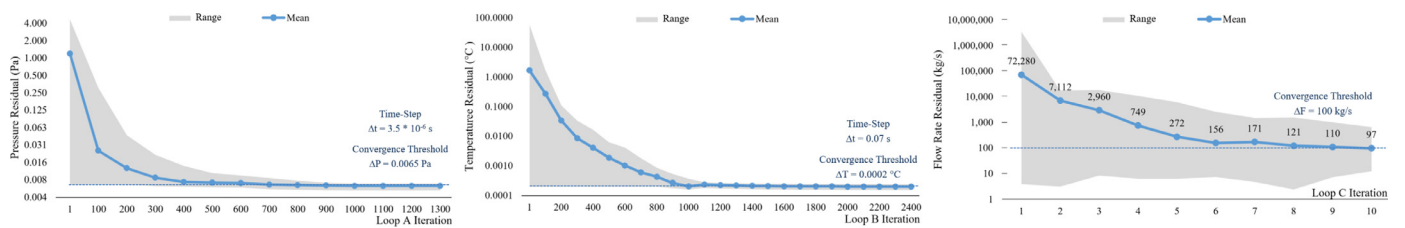

Fig. 27. Convergence performance for Loop A (Left), Loop B (Middle) and Loop C (Right). Mean residual values by interactions are calculated for a total of 30 days (720 h) in both winter (Dec. 7-26, 2014) and summer (Sept.4-23, 2015).

using a real urban neigbhhorhood:

- The scope and duration of evaluation studies are limited. The current field measurement was conducted in one urban neigobhrood – Sai Ying Pun, Hong Kong; the duration of studies covered daytime hours in two days; measurement in evening hours were missing due to logistic limitations.
- The number of measurement locations in the field studies were confined to four at the ground level; Limits in both manpower and equipment available reduced the number of concurrent measurement allowable; safety considerations prohibited the hanging of equipment from building balconies in order to obtain vertical temperature profiles above street canyons.

- Means of urban surface temperature measurement were to be improved. The authors acknowledge that infrared camera exhibit considerable uncertainties in the measurement of surface temperature; this shortcoming, despite practical difficulties in accessing private building estates, is expected to be addressed in further evaluation studies planned in the next steps.

To address the above limitations, the follow studies are planned for the next steps:

- Further evaluation studies are to be conducted on a 1:50 mockup site consisted of buildings made of concrete bins; the idea is to introduce artificial heat source of known power outputs to mimic traffic exhaust and building HVAC exhaust. This al-

lows more precise control of anthropogenic heat outputs compare with field studies in a real urban neighborhood; On the mock-up site, it will be feasible to precisely measure surface temperature using thermocouples and to measure the vertical temperature profiles in street canyons.

- To develop model components allowing assessment of winter heating. To this aim, appropriate assumptions are to be made on set points and COP for heating.
- Further studies are planned to include plants and moisture modules to estimate latent heat transfer. Outcomes can allow assessment of the impact of urban greenery, i.e. trees, lawns, and water features in their effectivevness in the mitigation of urban heat island effects.
- Tasks are scheduled to accelerate solver algorithms in order to allow annual-hour simulation for the model to assess building energy and microclimate conditions. This is expected to be conducted in the next steps of studies via (1) refinement of convergence critiera for practical purposes, (2) streamlining the data exchange between the UMM and BE components, which are currently written in two separate programming languages: Python & Fortran.

4. Conclusions

A coupled model for urban microclimate and building energy has been developed. Field measurements were conducted in a high-density neighbourhood in Hong Kong to evaluate the model performance. The major contributions of this research lie in the following:

First, an UrBEC model has been developed to describe the energy performance of a cluster of buildings in the context of the surrounding microclimate; the research has therefore contributed to the literature of environmental modelling at the scale of a cluster of buildings (50-500m) typical of which most buildings and urban design projects are commissioned. Simulation results show reasonable agreement with onsite measurement data in terms of air temperature and building surface temperature in both winter and summer.

Second, the simulation study for Sai Ying Pun, Hong Kong suggests that on average street canyons can experience temperature rise of 2 ℃ compared with the urban canopy layer in summer; the maximum warming effect is 4 ℃; the temperature variation across the neighbourhood can be 1-3 ℃. Building HVAC exhaust and traffic exhaust are the main causes of temperature rise in the street canyons; street level air is predicted to be 0.6 ℃ warmer than those at higher levels (20m +). Predicted building cooling demand is expected to increase up to 15 % in summer due to the varying temperature profiles in the neighbourhood.

Third, the UrBEC model has demonstrated potential values in support of early stage design. It can predict the distribution of temperature profile and building energy performance in a neigh-

bourhood for a given design layout; predicted solar radiation, surface temperature, airflow rate, and air temperature distribution can be used to assess the quality of thermal environments in pocket parks and streets. The model demonstrates satisfactory computing efficiency: it runs 5 times faster than the existing approach based on CFD methods, allowing simulation for an extended period and open up opportunities in supporting early-stage design and development decisions.

Declaration of Competing Interest

The authors declare to their best knowledge that there is no conflict of interest in regard to the research outcomes and findings from the manuscript submitted for publication.
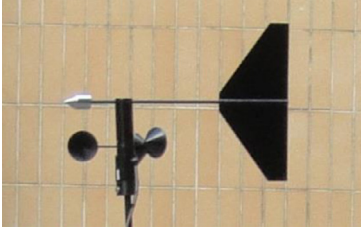
Acknowledgement

Appendix

The specifics of the portable HOBO weather station are provided as it is shown in Table 3: Temperature & RH sensor (U23 Pro v2 sensor)+Solar radiation shield (M-RSA), Wind Speed / Direction Smart Sensor (S-WCA-M003), Weather Station Logger (H21-001) and Radiation Sensor (S-LIB-M003).

Convergence conditions for the Re-Circulating Boundary are provided below: the results of mean zonal temperature at the model domain $\bar{T}_N$ as a function of time step N are plotted in Fig. 28. Data were computed from a 24 h cycle on Sept.5, 2015. $\bar{T}_N$ usually converges after 10 iterations, in which $\Delta \bar{T}_N$ drops below 0.02 ℃, the accuracy range of measurement sensors. After two steps, the domain mean air temperature increment from T_a as a percentage of the convergence value $(\bar{T}_N - \bar{T}_a)/(\bar{T}_\infty - \bar{T}_N)$, reaches 25%.

A comparison of technical parameters of the UrBEC model together with the other two approaches, Fluent-Solene (Bouyer et al., 2011) and ENVI-met-EnergyPlus (Yang et al.) is provided in Table 4 below. The UrBEC model appears to run faster than the other two.

Table 3
Specifies of portable HOBO weather stations and components used in this study.

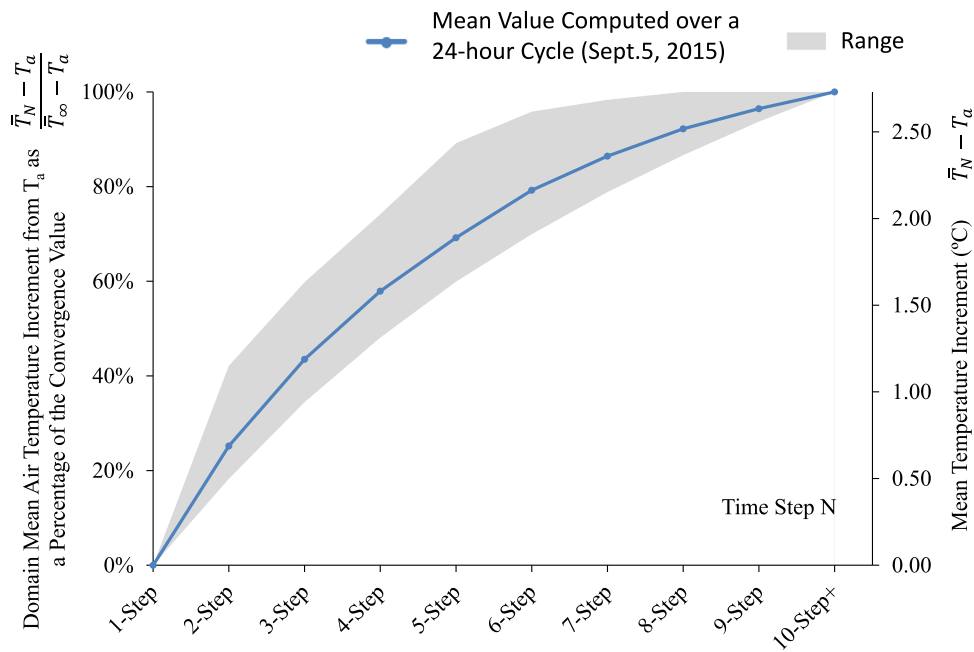| Temperature & RH sensor (U23 Pro v2 sensor)+Solar radiation shield (M-RSA), | Weather Station Logger (H21-001) | Wind Speed / Direction Smart Sensor (S-WCA-M003) | Radiation Sensor(S-LIB-M003) |

Fig. 28. Percentage changes of mean zonal temperature at the model domain $\bar{T}_N$ as a function of time step N used in the Re-Circulating Boundary computation.

Table 4
A comparison between UrBEC model and two other CFD-based approaches.

Technical Parameters	Fluent + Solene (Bouyer et al. [10])	ENVI-met + EnergyPlus (Yang et al. [13])	UMM + HTB2 (Huang et al., 2019)
Running Time (per hour of simulation run)	~60 mins*	~300 mins**	10 mins
Size of Case Project	1120 m × 1520 m × 180 m	150 m × 150 m × 50 m	252 m × 378 m × 100 m
# of Air Cells (external zones)	1,725,000	140,625	194
# of Buildings	11	15	44
Surface Mesh	1545 (Surface Mesh)	~100 (Linking Unit)***	835 (Surface Element)

* Estimated based on 164 h for a full thermoradiative and CFD coupling for a simulation period of one week.

** Estimated based on 168 h for a simulation period of three days.

*** The number of linking unit, the surface connecting a building space to external environment, was not specified in the orginal manuscript. An educated estimate of 100 was made according to the schematic depiction in Fig. 3.

References

[1] J. Nichol, Remote sensing of urban heat islands by day and night, Photogramm. Eng. Remote Sens. 71 (2005) 613–621, doi:10.14358/PERS.71.5.613.

[2] J. Huang, C. Zhou, Y. Zhuo, L. Xu, Y. Jiang, Outdoor thermal environments and activities in open space: an experiment study in humid subtropical climates, Build. Environ (2016), doi:10.1016/j.buildenv.2016.03.029.

[3] M.S. Wong, J. Nichol, E. Ng, A study of the "wall effect" caused by proliferation of high-rise buildings using GIS techniques, Landsc. Urban Plan 102 (2011) 245–253, doi:10.1016/j.landurbplan.2011.05.003.

[4] K.L. Lau, E. Ng, An investigation of urbanization effect on urban and rural Hong Kong using a 40-year extended temperature record, Landsc. Urban Plan 114 (2013) 42–52, doi:10.1016/j.landurbplan.2013.03.002.

[5] D.B. Crawley, L.K. Lawrie, F.C. Winkelmann, W.F. Buhl, Y.J. Huang, C.O. Pedersen, R.K. Strand, R.J. Liesen, D.E. Fisher, M.J. Witte, J. Glazer, EnergyPlus: creating a new-generation building energy simulation program, Energy Build. 33 (2001) 319–331, doi:10.1016/S0378-7788(00)00114-6.

[6] L. Yang, B.-J. He, M. Ye, Application research of ECOTECT in residential estate planning, Energy Build. 72 (2014) 195–202, doi:10.1016/j.enbuild.2013.12.040.

[7] D.B. Crawley, J.W. Hand, M. Kummert, B.T. Griffith, Contrasting the capabilities of building energy performance simulation programs, Build. Environ. 43 (2008) 661–673, doi:10.1016/j.buildenv.2006.10.027.

[8] B. Bueno, L. Norford, J. Hidalgo, G. Pigeon, The urban weather generator, J. Build. Perform. Simul. 6 (2013) 269–281, doi:10.1080/19401493.2012.718797.

[9] J. Arnfield, Two decades of urban climate research: a review of turbulence, exchanges of energy and water, and the urban heat island, Int. J. Climatol 23 (2003) 1–26, doi:10.1002/joc.859.

[10] J. Bouyer, C. Inard, M. Musy, Microclimatic coupling as a solution to improve building energy simulation in an urban context, Energy Build. 43 (2011) 1549–1559, doi:10.1016/j.enbuild.2011.02.010.

[11] Q. Chen, J. Srebric, Application of CFD tools for indoor and outdoor environment design, Int. J. Archit. Sci 1 (2000) 14–29.

[12] M. Bruse, H. Fleer, Simulating surface–plant–air interactions inside urban environments with a three dimensional numerical model, Environ. Model. Softw. 13 (1998) 373–384, doi:10.1016/S1364-8152(98)00042-5.

[13] X. Yang, L. Zhao, M. Bruse, Q. Meng, An integrated simulation method for building energy performance assessment in urban environments, Energy Build. (2012), doi:10.1016/j.enbuild.2012.07.042.

[14] M. Bruse, H. Fleer, Simulating surface-plant-air interactions inside urban environments with a three dimensional numerical model, Environ. Model. Softw. 13 (1998) 373–384.

[15] A. Novoselac, J. Srebric, A critical review on the performance and design of combined cooled ceiling and displacement ventilation systems, Energy Build. 34 (2002) 497–509, doi:10.1016/S0378-7788(01)00134-7.

[16] L. Yang, Y. Li, City ventilation of Hong Kong at no-wind conditions, Atmos. Environ 43 (2009) 3111–3121, doi:10.1016/j.atmosenv.2009.02.062.

[17] D. Robinson, F. Haldi, J.H. Kämpf, P. Leroux, D. Perez, A. Rasheed, U. Wilke, CITYSIM: comprehensive micro-simulation of resource flows for sustainable urban planning, in: Proceedings of the International IBPSA Conference, IBPSA, Glasgow, 2009, pp. 1083–1090.

[18] R. Christoph F, D. Timur, J.J Alstan, R. Tarek, S. Andrew, Umi - an urban simulation environment for building energy use, daylighting and walkability, in: Proceedings of the BS2013 13th Conference of the International Building Performance Simulation Association, 2013, pp. 476–483.

[19] DesignBuilder Software Ltd, DesignBuilder Software Packages, (2019). https://designbuilder.co.uk/ (accessed August 23, 2019).

[20] J. Huang, P. Jones, R. Peng, X. Li, S. Hou, H. Kong, An integrated model for urban microclimate and building energy in high-density cities for early stage design, in: Proceedings of the Building Simulation, IBPSA, San Fran, 2017, pp. 1586–1593.

[21] Trimble Inc., SketchUp, (2016).

[22] P. Jones, S. Lannon, X. Li, T. Bassett, D. Waldron, Intensive Building Energy Simulation At Early Design Stage, in: Proceedings of the BS2013 13th Conference of the International Building Performance Simulation Association, 2013.

[23] J. Huang, A. Zhang, R. Peng, Evaluation the MultiZone Modle for Street Canyon Airflow in High-Density Cities, in: Proceedings of the 14th Conference of the International Building Performance Simulation Association, Hyderabad, India, 2015.

[24] M. Musy, E. Wurtz, F. Winkelmann, F. Allard, Generation of a zonal model to simulate natural convection in a room with a radiative/convective heater, Build. Environ. 36 (2001) 589–596, doi:10.1016/S0360-1323(00)00043-3.

[25] R. Rao, Q. Luo, B. Li, A simplified mathematical model for urban microclimate simulation, Build. Environ. 46 (2011) 253–265, doi:10.1016/j.buildenv.2010.07.019.

[26] W. Liang, J. Huang, P. Jones, Q. Wang, J. Hang, A zonal model for assessing street canyon air temperature of high-density cities, Build. Environ. 132 (2018) 160–169, doi:10.1016/j.buildenv.2018.01.035.

[27] ASHRAE, ASHRAE Handbook: Fundamentals, ASHRAE, Atlanta, GA, 2013 2013.

[28] Oscar Faber and Partners, IEA Annex 1 Computer Modelling of Building Performance: Results and Analyses of Avonbank Simulation, Oscar Faber and Partners, 1980.

[29] K.J. Lomas, H. Eppel, C. Martin, D. Bloombield, Empirical validation of detailed thermal programs using test room data, 1: Final Report, 1994.

[30] J. Neymark, R. Judkoff, D. Alexander, P. Strachan, A. Wijsman, in: IEA BESTEST Multi-Zone Non-Airflow In-Depth Diagnostic Cases, 12th IBPSA, Sydney, 2011, pp. 14–16. http://www.nrel.gov/docs/fy12osti/51589.pdf.

[31] P.T. Lewis, D.K. Alexander, HTB2: A flexible model for dynamic building simulation, Build. Environ. 25 (1990) 7–16, doi:10.1016/0360-1323(90)90035-P.

[32] EMSD, Residential air conditioning: an energy efficiency guide, Hong Kong, 2015. https://www.emsd.gov.hk/filemanager/tc/content_718/EMS_Energy(low-res).pdf.

[33] K.S. Lam, D.W.T. Chan, E.H.W. Chan, C.T. Tai, W.Y. Fung, K.C. Law, Infiltration of outdoor air in two newly constructed high rise residential buildings, Int. J. Vent. (2006), doi:10.1080/14733315.2006.11683742.

[34] S.K. Wong, K.W. Chau, Y. Yau, A.K.C. Cheung, Property price gradients: The vertical dimension, J. Hous. Built Environ. (2011), doi:10.1007/s10901-010-9203-8.

[35] H. Taha, Urban climates and heat islands: albedo, evapotranspiration, and anthropogenic heat, Energy Build. (2002), doi:10.1016/s0378-7788(96)00999-1.

[36] W. Wang, W. Zhou, E.Y.Y. Ng, Y. Xu, Urban heat islands in Hong Kong: statistical modeling and trend detection, Nat. Hazards. (2016), doi:10.1007/s11069-016-2353-6.